CHALMERS
UNIVERSITY OF TECHNOLOGY

RI.
SE

Research Institutes
of Sweden

Production of Cellulose Templated Mesoporous Silica Using Fibre Spinning

Master's Thesis in Biotechnology

Daniel Schmidt

DEPARTMENT OF CHEMISTRY AND CHEMICAL ENGINEERING
Division of Applied Chemistry

CHALMERS UNIVERSITY OF TECHNOLOGY
Gothenburg, Sweden 2020-02-12
www.chalmers.se

Abstract

Silica (or silicon dioxide, SiO_2) occurs in abundance in nature, e.g. as the main constituent of sand, and there are many different existing uses for this material such as enzyme immobilisation, drug delivery and chromatography. There are also potential novel applications. This makes silica a very interesting and promising material to study more closely. For chromatographic purposes silica must be porous and more specifically mesoporous, i.e. with a pore size between 2 and 50 nm. The objective of this master thesis was to produce silica in this mesoporous state. As stated in the beginning of this paragraph one of the uses of mesoporous silica is to immobilise enzymes in the mesopores. By immobilising enzymes their stability can be increased and the cost, compared to using enzymes in their native form, can be reduced. Also, as mentioned, another application for mesoporous silica is for drug delivery by filling the pores with drugs that can then be transported into cells through endocytosis. If the pores instead of drugs are filled with e.g. a fluorescent dye the silica can aid in the identification of certain cell types.

One possible way to produce mesoporous silica is to use a fibre spinning approach. However, since silica can not be spun alone additives are needed. The additive that was used was cellulose nanocrystals (CNC) or cellulose nanofibres (CNF). In this master's thesis the properties and gelling behaviour of many different SiO_2/CNC and SiO_2/ CNF mixtures were studied to get a better understanding on how these materials interacted. From bulk gelling experiments it could be concluded that there was a clear synergy effect between CNC and silica where non-gelling samples of CNC and silica formed stable gels rapidly after being mixed at various pHs. The findings from these experiments were helpful later in the work when studying extrusion into a gelling bath.

The gelling behaviour when extruding various CNC/silica mixtures into different gelling baths using a syringe and a needle was also explored. Subsequently, the fibre forming properties of the mixtures were examined to further understand the properties of the formed fibres; both on a physical macroscopic scale and later on a microscopical scale using Scanning Electron Microscopy (SEM) and nitrogen sorption analysis using the Brunauer-Emmett-Teller (BET) method. These analyses were conducted to get an understanding of the surface of the samples as well as data about their porosity.

In terms of mechanical stability it could be concluded that fibres composed of CNC and silica were generally very brittle whereas fibres with CNF and silica were generally robust. SEM analysis showed that fibres composed of CNC and silica did not produce highly porous fibres after calcination. This means that CNC is unsuitable as a template for producing mesoporous silica. Nitrogen sorption analysis was also used to study the surface area, pore volume and pore size of the (porous) silica. Overall, sorption analysis showed that the silica mixed with CNC did not produce very porous silica fibres after calcination. However, using CNF resulted in a much more porous silica after calcination with a surface area of 205 m^2/g (sorption data). These values can be compared to the surface area of the pure silica used which was 123 m^2/g. These results show that silica/CNF mixtures can be spun into stable enough fibres that upon drying and calcination can form a mesoporous silica material.

Acknowledgements

I would like to thank everyone that have been of great help during this master's thesis. Thank you Kinga Grenda for all your help with the nitrogen sorption analysis. Thank you to Mats Hulander for helping me set up the pH measurements and for helping me with the calcination oven. Thank you to Victor Eriksson for your company in the laboratory and for our many discussions.

A massive thank you to my deputy supervisor Archana Samanta for always taking time answering my questions and helping me out when I was running back and forth between the laboratory and your office.

Thank you to Romain Bordes for your supervision and helping me see the big picture of this project answering so many of my questions.

Thank you to Lars Nordstierna for your examination of this master's thesis.

Thank you to Hanna Ulmefors at RISE for helping me run a seemingly endless number of SEM samples and for all the great support. Also thank you to Oleksandr Nechyporchuk for your help and with the fibre spinning.

Finally, a massive thank you to my family and friends for all your invaluable support during this project and in general.

Gothenburg, February 2020

Daniel Schmidt

Abbreviations

AFM - Atomic Force Microscopy
BED - Backscattered Electron Detector
BET - Brunauer-Emmett-Teller
CNC - Cellulose Nano Crystals
CNF - Cellulose Nano Fibres
EDS - Energy-Dispersive X-ray Spectroscopy
LED - Lower Electron Detector
MCC - Micro-Crystalline cellulose
SEM - Scanning Electron Microscopy
SNP - Silica Nano Particle

1 Introduction

1.1 Background

The world is facing several difficult environmental challenges. Historically and still today many harmful chemicals are being used and released into nature. Many improvements have been made with a shift towards expansion of renewable energy sources and more environmentally friendly materials but there is still a lot of progress to be made. With a growing population the need for new sustainable production methods for existing materials is paramount to be able to secure a prosperous future for the planet and its inhabitants. With these challenges in mind, this project will explore a new more environmentally friendly process to produce a porous silica material with many different applications, e.g. in separation columns for chromatography and for drug delivery.

Silica occurs in abundance in nature and there are many different applications for e.g. mesoporous silica. This makes silica a very interesting and promising material to study more closely. One of all the applications is to immobilise enzymes in the mesopores. By immobilising enzymes their stability can be increased and the cost, compared to using enzymes in their native form, can be reduced. Mesoporous silica is also used in separation columns during chromatography. Traditionally, mesoporous silica for separation columns has been produced using the emulsion solvent evaporation technique or by the self-assembly of a structure directing agent based on polymer or surfactant systems. Mesoporous silica particles have also been prepared in a water/oil phase by using an organic templating method. By using this method both the inner pore size of the material and outer diameter of the particles could be controlled successfully. The new wet-spinning process that will be explored in this project could provide an opportunity to replace these processes with a bio-based alternative that is more environmentally friendly. Mesoporous silica-based materials have other practical applications in biotechnology and biomedicine and recent studies have shown that mesoporous silica nanoparticle materials can be used to improve membrane permeability and biocompatibility.

1.2 Aim

The aim of the work in this master's thesis is to study if cellulose can be used as an aiding structure directing agent for silica in a wet-spinning process. The end goal is to produce a mesoporous silica with a pore size that is very well defined. This silica could then be used in e.g. separation columns during chromatography or for drug delivery in pharmaceutical applications. The produced silica could be able to challenge existing materials when it comes to performance and pricing.

1.3 Limitations

The project will focus on two types of cellulose: Cellulose NanoCrystals (CNC) and Cellulose NanoFibres (CNF). Other types of cellulose such as MicroCrystalline Cellulose (MCC) or regenerated cellulose will not be considered.

Only one type of silica will be used: bare colloidal silica nano particles (Levasil CS30-236). There are many other types of colloidal silica but these will not be considered.

The final material (silica) will be characterised using Scanning Electron Microscopy (SEM) to determine the structure of the material and nitrogen sorption analysis with the BET (Brunauer-Emmett-Teller) method was used to determine the surface area, pore volume and pore size of the (porous) silica. Physical material properties such as tensile strength and compressive strength of the fibres will not be examined.

1.4 Method

The project was separated into four different stages with different areas of focus to reach the goals of the study.

The first step was to study the gelling behaviour of different SiO_2/CNF mixtures. Gelling experiments were performed to see if and how these mixtures gelled when being mixed at different ratios at different pH in small vials. The gelling behaviour of pure silica and pure CNC was also examined. The bulk gelling experiments were conducted to get an initial understanding of how mixtures of silica and CNF interacted.

The second stage focused on studying the gelling behaviour when manually extruding the mixtures into different gelling baths using a syringe and a needle. At this stage the fibre forming properties of the mixtures were also examined to further understand the properties of the formed fibres; both on a physical macroscopic scale and later on a microscopical scale using SEM and nitrogen sorption analysis

The third stage was to calcinate the samples to remove the cellulose and other materials/ impurities from the samples and be left with only the (porous) silica.

The fourth step was to examine the calcined samples using nitrogen sorption analysis to study the surface area, pore volume and pore size of the (porous) silica.

2 Theoretical background

2.1 Mesoporous silica

The porosity of materials can be defined as follows: microporous with a pore size of less than 2 nm, mesoporous with a pore size of 2-50 nm and macroporous with a pore size of more than 50 nm [1]. The focus of this project will be on mesoporous silica due to its pore size making it suitable for the considered applications of this project.

It is possible to extract bio-based silica, e.g. from rice husk. In that case, the surface area of the extracted silica is strongly dependent on the pH during the extraction procedure. With increasing pH the surface area decreases. A study showed that the largest surface area was obtained at a pH of 3 [2].

There are many different preparation methods for mesoporous silica materials. Silica can be produced in the form of e.g. films, spheres, fibres or in bulk form. As for mesoporous silica, it can be produced using an organic template-driven synthesis process. These methods are used in large scale in industry but there are several drawbacks e.g. the use of harmful chemicals such as hydrazine (N_2H_4) or ammonia (NH_3) as catalysts [3], [4]. Traditionally, mesoporous silica for separation columns has been produced using the emulsion solvent evaporation technique or by the self-assembly of a structure directing agent based on polymer or surfactant systems. As mentioned in the background section, mesoporous silica particles have also been prepared in a water/oil phase by using an organic templating method. An important advantage of using this method is that both the inner pore size of the material and outer diameter of the produced particles can be tailored [3].

The number of different applications for mesoporous silica are vast. Mesoporous silica can for example be used for enzyme immobilisation. By immobilising enzymes in (mesoporous) silica the costs compared to using enzymes in their native form can be reduced by increasing the operational stability of the enzymes [5]. Mesoporous silica-based materials have other practical applications in biotechnology and biomedicine and recent studies have shown that mesoporous silica nanoparticle materials can improve membrane permeability and biocompatibility [6]. Mesoporous silica is also used in columns for HPLC (high performance liquid chromatography)]. In these columns the surface area of the chromatographic substrate is important. In LC the separation occurs between the liquid phase and the solid phase. Thus, the larger the surface area of the solid phase, the better the separation [7]. Mesoporous silica has also been used in capillary gas chromatography [8].

2.2 The structure of cellulose

Cellulose is the main component of the cell walls of (higher) plants. This makes it the most abundant organic polymer and also a very important one [9]. In nature, cellulose often exists together with lignin and other polysaccharides e.g hemicelluloses and pectins and also with small amounts of organic compounds such as extractives [10].

The chemical formula for cellulose is $(C_6H_{10}O_5)_n$ and it consists of repeating subunits of anhydroglucose. These subunits are linked by β-1-4-glycosidic bonds seen in Figure 1.

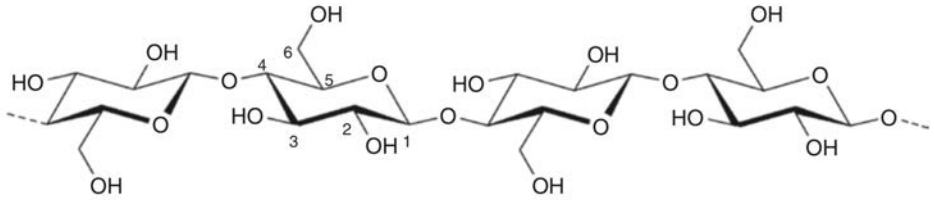

Figure 1. Cellulose polymer constructed of linked anhydroglucose subunits [11].

The subunits alternate turning around the longitudinal axis of the cellulose chain. Therefore, the repeating unit of cellulose can be seen as two andhydroglucose units [9]. Each anhydroglucose monomer contains three hydroxyl groups of two different types, one primary on carbon 6 and two secondary on carbon 2 and 3 respectively [12].

Because of the propensity of cellulose to self-order there are several structural levels of cellulose. These different levels are represented in Figure 2:

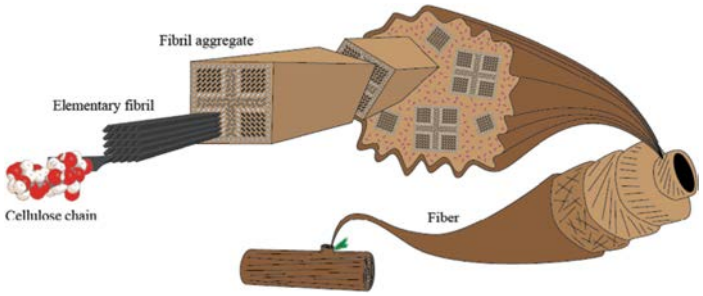

Figure 2. The hierarchical structure of cellulose. (Courtesy of Alexander Idström)

Firstly, the cellulose chains arrange themselves into elementary fibrils. These have regions of varying degree of order. Secondly, the fibrils arrange themselves into fibril aggregates; structures of higher order producing layers of varying density and texture. The fibril aggregates arrange themselves in varying angles to each other eventually producing macro fibres present in e.g. wood. This complex structure of cellulose and the fibres it can arrange into defines different properties of cellulose such as its mechanical properties.

2.3 Nanocellulose

There are typically two different types of nanocelluloses that are distinguished; cellulose nanocrystals (CNC) and cellulose nanofibres (CNF) that can be produced from a top-down apporach. They differ in their structure and properties but also in the way they are produced. Generally, CNC is produced by acid treatment and CNF is produced by mechanical disintegration [13]. The two different types of nanocelluloses will now be discussed in further detail.

CNC is produced by removing the amorphous regions naturally occurring between the crystalline regions of the cellulose [14]. This is done by using sulphuric acid and results in the production of homogenous crystallites. These crystallites are regularly referred to as sulfonated CNC [15].

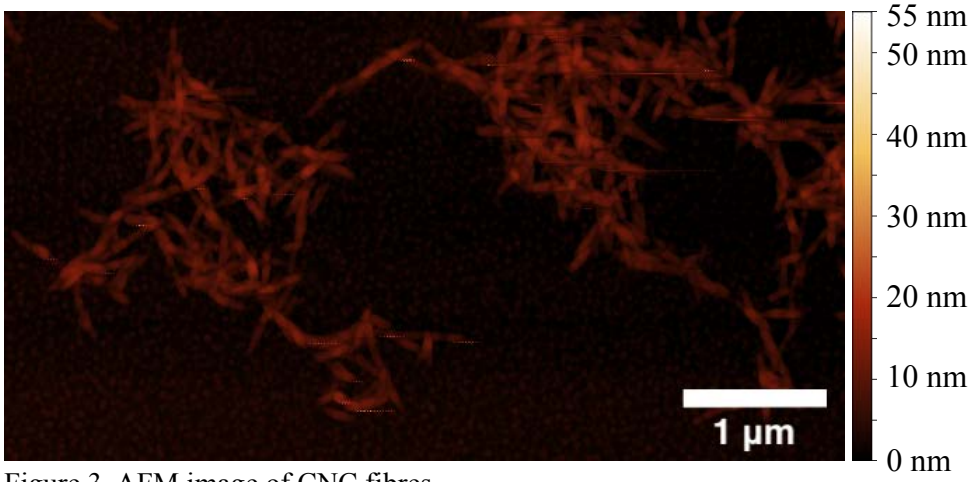

Figure 3. AFM image of CNC fibres.

As can be seen in Figure 3 the crystalline particles in CNC are stiff, rod-like and have dimensions below 1 µm. For CNC that has been produced from pulp typical dimensions are 3-5 x 100-200 nm. The high interest in these nano-crystals is due to their properties such as high surface area, low density and high mechanical strength. CNC also forms stable suspensions in water and other mediums [14].

Acid hydrolysis is a suitable method for synthesising CNC from pulp or from microcrystalline cellulose (MCC). The synthesis uses sulphuric acid which provides anionic sulfate esters that gives the particle a negative charge that enables electrostatic stabilisation [16]. Nanocrystalline materials have a larger surface area and more well-defined particles than microcrystalline materials [17].

CNC and CNF can be obtained from trees and plants. These are built of microfibrils which in turn are built from bundles of nanofibrills. As can bee seen in comparing these two AFM images, the CNF fibres are much longer than the CNC fibres.

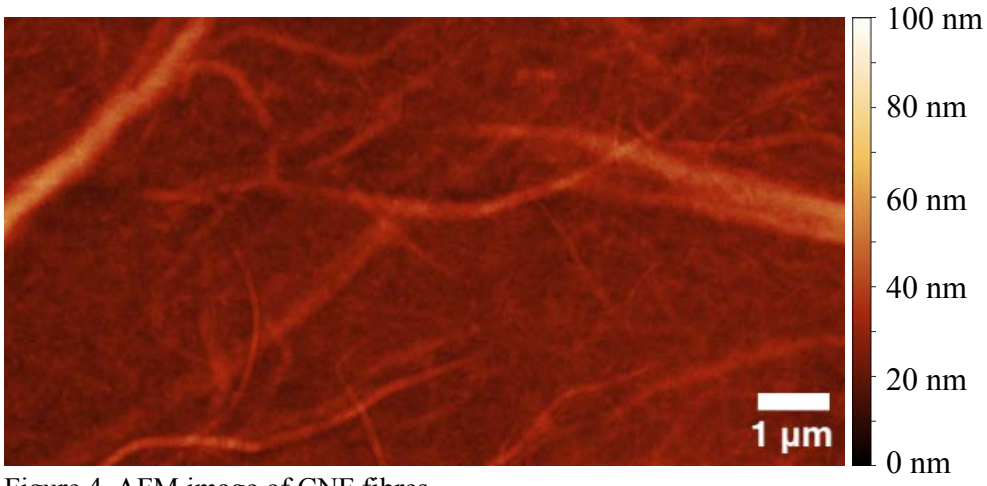

Figure 4. AFM image of CNF fibres.

By separating these nanofibrills from the wood, by using mechanical force, dispersions of CNF can be made. These CNFs are usually a few micrometres long and 5 nm in diameter [18]. The CNF fibrils can be seen in Figure 4. This means that the CNF are much longer than the CNC and this has a significant impact on the properties of the different materials. In contrast to CNC, CNF has both crystalline and amorphous regions [18]. The filaments of CNF are flexible. As can be seen in Figure 4 they occur both as individual fibres and as bundles of several fibres.

2.4 Gelling of CNC and CNF

CNC has a negative surface charge in water that enable the formation of stable suspensions. For colloidal particles in suspensions in water the separation and stability can be explained using DLVO theory. There are two types of forces acting on the particles; attractive van der Waals forces and repulsive interparticle forces [15].

Regardless of whether the interactions are between colloidal particles or suspensions of CNC rods they can be examined in terms of colloidal stability. As for the interactions between the CNC rods they are highly dependent on the orientation of the rods [15]. Again, there are two types of forces that can be considered; attractive and repulsive. There is the regime with high ionic strength in which attraction dominates, due to shielding of the negative surface charges, and the regime with low ionic strength where repulsive forces dominate. When the ionic strength is low the CNC rods form stable isotropic suspensions. At this lower ionic strength a phase separation occurs with an anisotropic lower phase and an isotropic upper phase [15]. If the ionic strength is high, attractive van der Waals forces dominate the interaction between the CNC rods and the double layer around them is compressed. Due to these forces, the CNC rods can form an isotropic gel [15]. The gelling of CNC can also be affected by the addition of a salt e.g. NaCl or $CaCl_2$.

2.5 Gelling of colloidal silica

At a pH between 2 and 11 the surface of silica is negatively charged [19]. Figure 5 shows the surface of a colloidal silica nanoparticle.

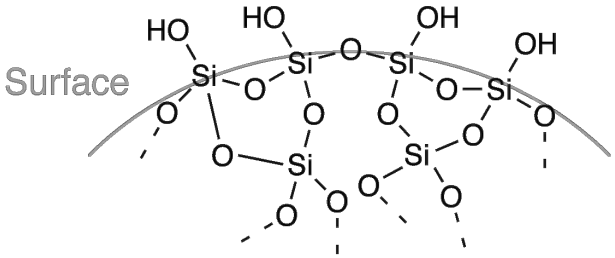

Figure 5. The surface of a silica particle with its hydroxyl groups.

If silica particles with sufficiently low surface charge come in contact with each other irreversible siloxane bonds that hold them together are formed between them [20]. The formation of these bonds is dependent on presence of hydroxyl ions (HO^-). A lower pH of a solution means a lower concentration of HO^- ions which generally leads to more gelling. This means that the gelling behaviour of silica is highly pH dependent. This behaviour can be seen in Figure 3 and will now be discussed in further detail.

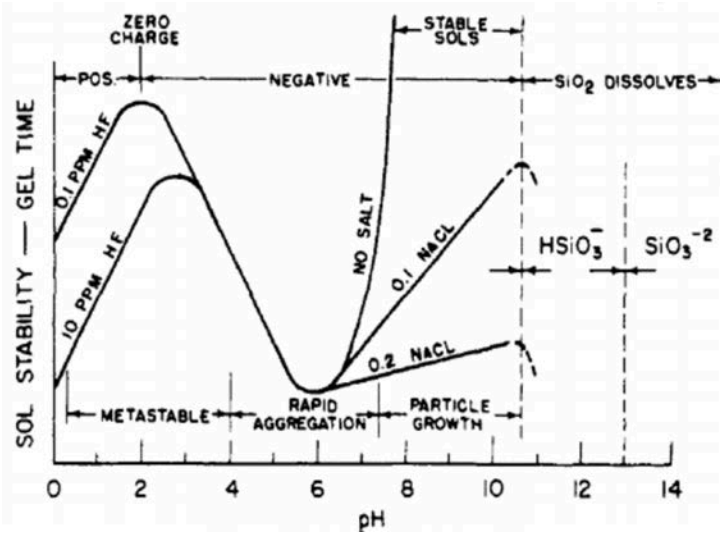

Figure 6. The pH dependence of the gelling behaviour of a colloidal silica-water system [20].

In Figure 6 three different regions can be observed. The first of these regions is between a pH of just above 0 and 4. In this region metastable gels can form. The second region occurs between a pH of 4 and 7.5. In this region the there is a rapid aggregation between the colloidal silica particles and the gel becomes much more stable. In the last region for a pH between 7.5 and 11 stable sols can be obtained. Overall, the aggregation is highly dependent on the presence or absence of salt (NaCl). As discussed earlier regarding CNC, silica also often has a negative surface charge. The surface charge of silica nanoparticles and the aggregation and gelling behaviour of these depend on both ionic effects and salt effects [19].

If the concentration of hydroxyl ions at the surface is increased the gel time also increases [19]. This becomes evident in studying the reduction in gel time when in the range where pH increases from 3-5. Worth remembering is that the concentration of hydroxyl ions increases as the pH increases and the suspension becomes less acidic. At silica surfaces there is a repulsive hydration layer present [21]. If the pH value of a suspension containing silica increases the capacity for forming hydrogen bonds at the surface decreases. This is due to the deprotonation of the silanol groups at the surface [22].

At a pH higher than 6 the hydroxyl concentration [HO^-] is no longer the factor that limits the rate of gelling. Instead, the rate of gelling is now controlled by the fact that the increasing charge of the particles leads to them repelling each other [20]. The result of this is that the aggregation rate and subsequently the gelling now decreases with increasing pH. A lower value on the y-axis means a shorter gel time, i.e. the silica gels most rapidly at around pH 6.

If there is an absence of salt (NaCl) the gelling time goes towards infinity in the region from pH 6 and up. This means that the silica solution is stable and does not aggregate to form a gel [20]. However, if there is a presence of salt the gel time increases slowly with increasing pH from 6 and up. Hence, the lower the salt concentration the longer the gel time. Between a pH of 0 and 3 the gel time increases with an increase in pH. This is due to the fact that nearly all silicas contain trace amounts of fluoride ions [20]. These fluoride ions enable the aggregation and gelling and as their concentration decreases with an increase in pH the predisposition for gelling decreases.

2.6 Gelling of a mixture of cellulose and silica

The interactions between cellulose and their influence on the gelling properties of the different mixtures is important to consider. As shown in Figure 2, silica nano particles (SNPs) have hydroxyl groups on their surface. One study has shown that for silica nanoparticles to form a cross-linked network it should adsorb two or more polysaccharides, e.g. cellulose. The same study also showed that if the concentration of silica nanoparticles is increased the gel strength also increased. This was up to a certain point after which an increase in concentration started to impair the gelling [24]. It has been demonstrated that adding SNPs to a solution containing hydroxyethyl cellulose (HEC) made the solution more viscous [23]. This means that the formation of a hydrogel can be induced by adding silica to a cellulose solution. The increase in viscosity may be due to HEC adsorbing to SNPs. Further, it has also been shown that by adding nanoparticles into different polymers different properties can be enhanced. These can be mechanical properties, the polymer's dimensional stability and their thermal stability [23].

By mixing two different solutions of e.g. 1 wt% cellulose with a 50 wt% silica mixture a stable (hydro)gel can be formed. By adding more silica to a cellulose suspension it could be seen that the gel strength increased [23].

It has also been shown that increasing the concentration of silica nano particles with a diameter of 120 nm in a mixture with polysaccharides (κ-carrageenan) impairs the gelling. This is attributed to the particles' steric hindrance preventing chain aggregation between the

polymers and thereby impairing the gelling [24]. However, this effect does not hold true for larger (440, 560 and 860 nm) silica nanoparticles. For these larger particles an increase of their concentration leads to the formation of more stable gels when mixed with the same polysaccharides [24]. These gelling properties of mixtures of silica and cellulose will be explored in more detail in this report.

The message from this is that when considering mixtures of cellulose and silica many different aspects needs to be taken into consideration. A mixture is not likely to behave in a manner that is just a simple combination of the two constituents cellulose and silica, especially when the cellulose species is present in the form of nanocellulose.

2.7 Spinning techniques

Cellulosic and synthetic filaments are mainly produced by two main different categories of spinning techniques; wet and dry-spinning [25]. The focus of the project will be on wet-spinning but the two other types of solvent-spinning techniques are dry-spinning and dry-jet wet spinning. These different spinning techniques make use of either a dissolved or a molten precursor. A spinning dope produced by a precursor can then be extruded through a spinneret [25]. The next step is solidification which is achieved in different ways depending on the method used. In melt spinning the dope is cooled, in dry spinning the solvent is evaporated and in wet spinning the dope is precipitated in an antisolvent [25]. Another method is electrospinning in which a polymer solution is drawn by an applied electric field [26].

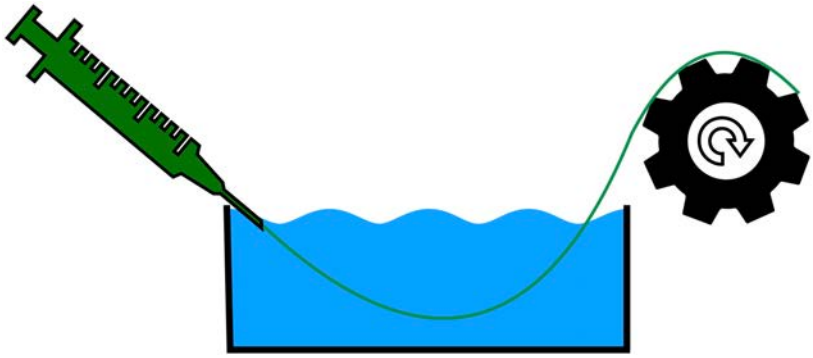

Figure 7. Schematic of the fibre spinning setup.

Figure 7 shows a wet spinning setup used in this project. The mixture in the syringe is extruded through the needle by an automatic syringe pump setup. As the mixture is extruded into the bath is gels. The formed fibres are then spun up onto a collection wheel to dry in room temperature. In the spinning of CNF the nanofibres are aligned in the spinneret. This alignment is due to the hydrodynamic shear within the spinneret. The alignment has been shown to increase the stiffness and tensile strength of the fibres and these properties can be enhanced even further by drawing of the fibres. Recent studies have also indeed shown that CNF can be spun into fibres with competitive mechanical properties [25].

2.8 Characterisation methods

2.8.1 Atomic Force Microscopy

Atomic Force Microscopy (AFM) can be used on insulating (non-conducting) samples [27]. In AFM the force between the tip of a small (450 μm) silicon cantilever and a surface is measured. A laser beam is reflected on the back of the cantilever. As the cantilever moves up and down when being scanned over the sample the deflection of the lever is detected by the laser [27]. Out of this information the structure of the surface is mapped.

In static mode, the distance and force between the surface is kept constant as the surface is mapped. As the tip distance to the surface is kept constant (constant force) the z-value to keep this constant distance correspond to the topography of the sample. The z-value is the value of the distance the cantilever is bent relative to its relaxed condition as the force from the sample is kept constant. In the static mode the atoms of the tip are in contact with the atoms of the sample [27].

AFM can also be run in dynamic mode where the cantilever is oscillating. This mode can also be referred to as the non-contact mode as the cantilever does not touch the surface. This method is gentler and therefore useful for e.g. biological samples where the surface potentially can be damaged by the strong repulsive forces between the tip and the sample present in the static mode [27]. As the cantilever gets close to the sample the resonance frequency response of the cantilever changes. This change can then be used as a detection signal to regulate the distance between the tip and the surface and to map the surface.

2.8.2 Electron Microscopy and Energy-Dispersive X-ray Spectroscopy

Two common types of electron microscopy are scanning electron microscopy (SEM) and transmission electron microscopy (TEM). Simplified, SEM can be viewed as a method that provides images of external topography. TEM, shows the internal structure of solids providing access to microstructural and ultrastructural details [28]. In other words, SEM can be used to analyse and get high resolution images many different types samples [29]. In this project SEM was used.

SEM works by creating an electron beam that is highly focused. This is achieved by emitting energetic electrons from an electron source. After the beam has been emitted from the source and accelerated to a high energy its diameter is reduced using different apertures and lenses [30]. The focused beam is then scanned in a pattern of discrete locations on the sample. Each of these locations results in two types of electrons emitting from the sample. These are backscattered electrons (containing most of their initial energy) and secondary electrons (with low kinetic energy) [30]. To ensure that the incoming electron beam as well as the scattered electrons do not encounter any other atoms that could cause unwanted scattering SEM is conducted in vacuum ($<10^{-4}$ Pa) [30]. The emitted signals are detected using either a secondary electron detector or a backscattered electron detector. There are several types of different detectors that are used in SEM. In this project both a lower electron detector (LED)

and a backscattered electron detector (BED) were used. The detected/measured signal is translated into a grey level for each individual location, creating the final SEM image of the sample [30]. The depth of focus in electron SEM is much larger than that in a light microscope. This can be attributed to the small aperture of the lens of the electron microscope and the wavelength of the electrons [29].

One useful future of SEM is that it can be used to give the elementary composition of a sample. This is made possible by the fact that the x-ray microprobe of the SEM is (almost always) equipped with an addition that enables the use of Energy-Dispersive X-ray Spectroscopy (EDS). The EDS can be used to rapidly provide an overview of the main elements that the sample is composed of. EDS is also simple to use since there is no focusing condition for the method. This means that the sample can vary several millimetres in hight without the results being affected [29].

2.8.3 Nitrogen sorption analysis

Nitrogen sorption analysis can be used to determine the surface area, pore volume and pore size of a sample [31]. The surface area of a subject is best described as the external surface area of a solid as well as the surface area of its pores. Determining the surface area using adsorption is a very powerful method as many other methods do not consider the porosity of the analysed material [32].

In nitrogen adsorption analysis a monolayer of nitrogen (other gasses are used as well) is physioadsorbed in a monolayer to the surface of a sample and from this coverage the surface area can be calculated using the BET equation. The Brunauer-Emmett-Teller (BET) equation is the most commonly used equation for this calculation. Physisorption is governed by weak van der Walls forces and it does not require much energy (1-2 kcal/mol) to remove the adsorbed molecules from the surface [32]. To adsorb at least a monolayer to the sample surface the temperature at which the experiment is conducted needs to be close to the boiling point of the inert gas i.e. 70 K for nitrogen [32]. To achieve such a low temperature the samples that are being analysed are lowered into a container with liquid nitrogen.

3 Experimental procedure

3.1 Materials

Here follows a complete summary of all the different chemicals that has been used in this project and their origins.

Levasil CS30-236 bare colloidal silica nano particles with a surface area of (360 m^2/g) from Nouryon AB was used for all the experiments involving silica. The silica was diluted with distilled water.

Ultra Cellulose Nano Crystals (CNC) was sourced from Celluforce, Canada.

Granular calcium chloride ($CaCl_2$) was obtained from Aldrich.

Hydrochloric acid (HCl) under a form of a 12 M solution was diluted to 1 M and 2 M solutions.

0.35 wt% CNF was used in all the experiments involving CNF. The CNF suspension was produced by RISE from a softwood sulphite dissolving pulp sourced from Domsjö Dissolving plus, Domsjö Fabriker AB, Sweden by carboxymethylation followed by fibrillation using a Microfluidizer M-110EH (Microfluidics Corporation, USA) for four passes.

3.2 Bulk gelling experiments

The initial gelling experiments were performed to see if and how a mixture of silica (SiO_2) and CNF gelled when mixed in different ratios at different pH for 2 ml volumes in 4 ml vials. The pH was measured after the addition of HCl to the vial. The pH of the samples was measured using a Jenway 3345 Ione Meter pH meter calibrated using three samples of known pH 4, 7, and 9.

After the desired pH had been reached for a sample, to quantify whether a sample had gelled or not at a specific pH, the vial was turned upside down to evaluate its gelling properties. If a sample had gelled enough to not fall down to the bottom of the vial it was considered as having gelled, passing the gelling test.

3.3 Gelling in bath using syringe extrusion

Initially, to study the gelling behaviour by extrusion, the silica/CNC mixtures were extruded into 4 ml or 20 ml vials using a 0.80 x 80 mm needle and a 2 or 5 ml syringe.

To study how and if the silica/CNC or the silica/CNF mixtures gelled in a bath in a dish with a 7 cm diameter. Extrusion was again done through a needle with 0.80 x 80 mm needle at a rate of approximately 0.02 ml/s from a 5 ml syringe using manual extrusion or later 3 ml/min by automatic extrusion using a syringe pump (New Era SyringeONE) and a 5 ml glass syringe.

The gelled samples were collected using spatulas of either 2 mm or 5 mm width. Alternatively the collection was done by pouring the mixture over a filter attached to a suction setup. The gelled silica/CNC or silica/CNF mixtures were then put into small 2 cm (diameter) beakers.

3.4 Calcination

The small beakers with the wet fibre/gel mixtures were put on a plate and put into the Nabertherm P 330 calcination oven were they were calcined at 600°C for 4 hours. The ramping up was done from room temperature (20°C) at a rate of 1.93°C/min (580°C/5 h). Two identical samples were gelled. One of them was calcined at 600°C and the other at 700°C but the duration of calcination was the same. This study was conducted to explore if the calcination temperature would have an impact on the final structure of the material. The

sample that was selected for calcination at these two temperatures was the 50 wt% silica/50 wt% CNC mixture.

3.5 Characterisation of calcined silica samples using SEM and EDS

To characterise the structure of the different silica dominated samples after calcination SEM was used. The SEM was done in a JSM-7800F SEM with the surface offset set to 5 mm. Prior to the SEM analysis, to avoid charge build-up on the surface, the samples were coated with palladium using the sputterer Emitech K550X. The sputterer was run for 3 minutes at 25 mA.

Alternatively, the samples were mounted on a SEM stub using carbon tape and sputtered with a 1.5 nm thin platinum layer. The samples were then analysed using a high-resolution SEM (JEOL JSM-7800F, JEOL,Peabody, US) operating at an accelerating voltage of 5 kV. The working distance was 4 mm for the microscopy and 10 mm for the EDS analysis.

3.6 Characterisation of calcined silica samples using nitrogen sorption analysis

To study the surface area, pore volume and pore size of the porous silica nitrogen sorption analysis was used. The samples were put for drying in the Micrometrics Smartprep for pretreatment at 90°C for 1 hour and then 200°C for 2 hours.The samples were cooled in a beaker containing liquid nitrogen during the measurements. The equilibrium interval for the measurements was set to 5 seconds. The isotherms for nitrogen adsorption/desorption were determined at 77.35 K. The relative pressure, p/p_0 increased from 0.0321 to 0.999 and then down to 0.0825. The calculated mass of the samples (after drying) was put into the system. The sorption analysis was left to run for 12 hours. The surface area, pore volume and pore size was determined using nitrogen sorption analysis in conjunction with the BET (Brunauer-Emmett-Teller) method.

4 Results and discussion

4.1 Bulk gelling experiments

The bulk gelling experiments were conducted to get an initial understanding on how silica and CNC or CNF interacts when being mixed at different ratios at different pHs. In this section the results of these experiments will be presented and discussed in further detail.

In the initial phase of this project the gelling behaviour of silica and CNC in a bulk setting was studied. These initial experiments were implemented to study if and how a mixture of silica (SiO_2) and CNC gelled when being mixed in different ratios at different pH (10, 8, 6, 4 or 2) in small (4 ml) vials. A small amount of HCl was added to one vial at the time and the pH was measured. After the targeted pH had been reached the vial was turned upside down to see if the sample had gelled or not. If the gel did not fall down to the bottom of the vial it had

gelled. This technique is sometimes referred to as the inverted test tube technique. It is a commonly used method to qualitatively determine the gelling state of a sample. It does, however have its drawbacks since it is strictly binary in its approach to whether a sample gels or not. It is therefore very important that quantitative data such as the dimensions of the container and the amount of sample are provided and considered [33]. This is because parameters such as these are likely to significantly impact the outcome of the inverted test tube technique. The reason for this is that the weight of the gel in relation to the dimensions of the vial is physical properties that determines (along with friction and other parameters) if the gel will fall down in the vial. One major benefit of the method is that it is rapid and efficient.

The time between when a sample had been lowered to the correct pH using HCl and being turned upside down was approximately 1 minute. However, the time was not continuously measured as the kinetics was not the main focus of these experiments. Not considering and measuring the time more closely was a decision made as it would have complicated the experiments. The reason for this is that the pipetting of HCl had to be done in several steps to reach the desired pH. Even in adding it in small increments (1 µl at a time) a tolerance of a pH of ± 0.2% was sometimes difficult to achieve. If the targeted pH was not achieved a new sample had to be prepared and the experiment repeated. More details on how much HCl was added to the samples and the concentration of the same see Table A.2 in Appendix. Even if it would be very difficult and time consuming to monitor the time more closely doing so might have led to a bit more accurate experiments. However, the difference was not considered likely to lead to a significantly different outcome. A couple of samples were on the border of being gelled and not and for these a restrictive approach was taken where a sample was rather considered non-gelling than gelling; i.e rather a false negative than a false positive.

Figure 8 shows a representation of significant aspects of the inverted test tube technique and the gelling behaviour of the samples. For the complete set of experiments please see Appendix: “2 Bulk gelling experiments”. Here follows the results from these gelling experiments.

Figure 8. Inverted test tubes with mixtures of 1 wt% CNC and 30 wt% silica.

Table 1. Weight percent of each component in its respective vial.

Sample	1	2	3	4	5	6	7	8	9	10	11
CNC [wt%]	1.00	0.90	0.80	0.70	0.60	0.50	0.40	0.30	0.20	0.10	0.00
Silica [wt%]	0.00	3.0	6.0	9.0	12.0	15.0	18.0	21.0	24.0	27.0	30.0

The samples in the picture were produced by mixing 1-0 wt% CNC with 0-30 wt% silica according to Table 1. The pH in all of these samples was 8.

These samples illustrates an interesting gelling behaviour; namely that there are two gelling zones for the mixture. The first gelling zone consists of sample 2-5. The samples have CNC concentrations ranging from 0.90 to 0.60 wt% and silica concentrations between 3.0 and 12.0 wt%. Although the samples are dominated by silica it is important to understand that neither of them would be gelling without the presence of CNC see Appendix: “2 Bulk gelling experiments”. This will be discussed in the next section as all the samples are summed up. The second gelling region consists of samples 8-11 where the gelling is dominated by the gelling properties of silica with 21-30 wt%. The reason that only this series of samples had dual gelling regions was that this was the only series of samples that ended with a 30 wt% silica concentration. It also had a starting CNC concentration of 1 wt% and pH of 8 which meant that not all of the samples of the series gelled.

A series of samples consists of 11 different points as seen in Table 1 where sample 1 contains only CNC and sample 11 contains only silica. There are many sets of 11 samples that either do not gel at any pH tested (pH 10, 8, 6 or 4) or only exhibit one gelling region. The reason why many samples exhibit one gelling region is that they do not contain samples with a very high silica content that could cause a second gelling region to occur. The series discussed earlier in this section is the only series of 11 samples that ended with a 30 wt% silica concentration for sample 11. Therefore, the gelling regions that these samples with lower maximum silica concentrations have regions where a synergy gelling between the silica and the CNC occurs.

To represent all the different silica/CNC mixtures and whether they gelled or not at a specific pH, two means of representing the data were selected. The first one was to use scatter plots to plot the samples in a concentration graph with the wt% of CNC in the sample on the y axis and the wt% of silica in the sample on the x axis. The second was to do a ternary plot where the relative wt% of silica, CNC but also water was represented.

First, the scatter plots will be presented and discussed.

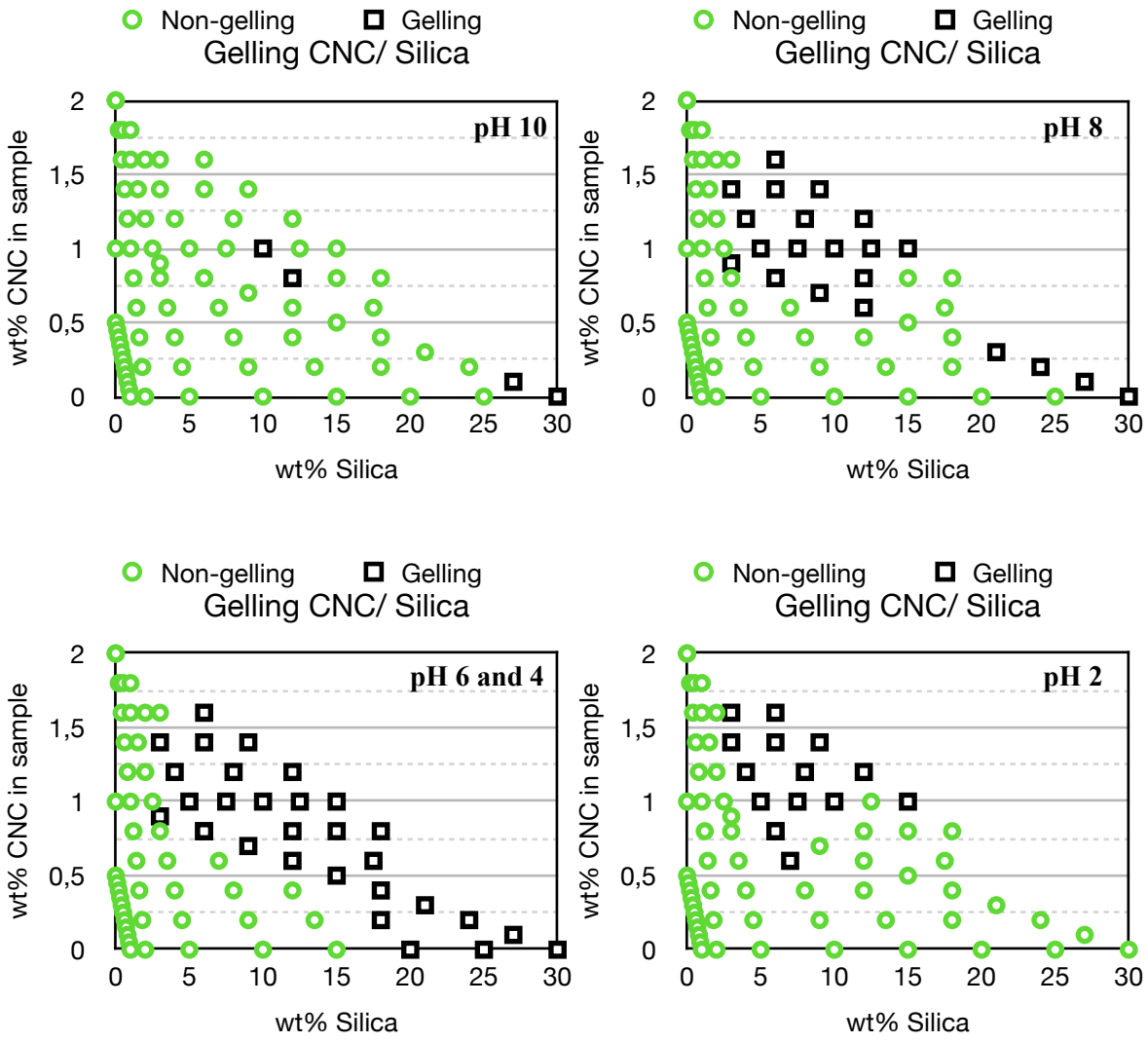

Figure 9. Scatter plots for silica/CNC mixtures at pH 10, 8, 6, 4 and 2. The green dots represents samples that have not gelled whereas the black squares represents samples that have gelled.

A benefit of using these scatter plots is that each individual sample can be identified easily. Initially, it is evident that there is some kind of synergy effect between silica and CNC because there are no samples that gel close to the x-axis without having a very high silica concentration. Upon just adding a small amount of CNC to a sample (i.e. moving up a bit on the y-axis) the gelling is much more prominent. This can for example be seen when studying the sample at pH 6 and 4 that have 10 wt% silica and 1 wt% CNC. This sample gels but when studying its corresponding samples with either pure silica (19 wt%) or pure CNC (1 wt%) neither of them gels. This clearly indicates that there very likely is some kind of synergy between silica and CNC. Another aspect that could be studied further is the kinetics of the gelling. Some of these samples may gel after a longer time period (several minutes or hours). However, in the scope of this project a very rapid gelling was considered necessary to select samples suitable for a continuous spinning process. It is also evident that pH plays a major role in whether a sample gels or not. This can be seen in Table 2.

pH	number of samples gelling	% of samples gelling
10	4	5.33
8	22	29.3
6 and 4	29 and 29	37 and 37
2	15	20.0

Table 2. Number of samples gelled at each pH.

Table 2 shows how many samples gelled at each pH. For pH 6 and 4 the samples that gelled were exactly the same. Both the amount and each specific sample. The most gelling occurs at a pH of 6 and 4 where the two gelling regions have merged into a larger one. These two gelling regions were the upper gelling region with less than 15 wt% silica and the lower gelling region with more than 20 wt% silica.

The gelling of silica has been described earlier in the theory section. The ability of silica to form hydrogen bonds decreases with increasing pH due to the deprotonation silanol groups at the surface [22]. In reverse this means that the ability for silica to gel increases with decreasing pH. In studying the gelling behaviour of the samples it can clearly be observed that a sample's ability to gel increases with a decrease in pH which is coherent with the theory. However, this is up to a point as at the lowest pH (pH 2 in this project) the gelling ability is decreased. This decrease in gelling ability was explained in the theory section and is due to the decreasing concentration of trace amounts of fluoride ions that catalyse the gelling with a decrease in pH between 0 and 3. The experimental data obtained is in agreement with these theoretical considerations.

One very important aspect of these gelling experiments is that most of the samples consist of a mixture of silica and CNC i.e. all samples that are not present on the x- or the y-axis of the scatter plots are mixtures of CNC and silica.

For the samples that only contain CNC it is evident that none of them (0.5 to 2 wt%) gel at any pH (pH 10 to 2). Pure silica at 30 wt%, however, gels at all the pHs but for pH 2. At pH 6 and 4 pure silica also gels at 20 and 25 wt%. Except from these few samples with a very high silica content that gel by themselves there it is evident that a synergy effect of silica and CNC is responsible for the gelling of the mixtures. There are no pure CNC samples that gel but there are several samples that only contain relatively low amounts of silica that do.

To compare the gelling behaviour of the different samples in an alternate manner ternary plots were made for the samples at the different pHs.

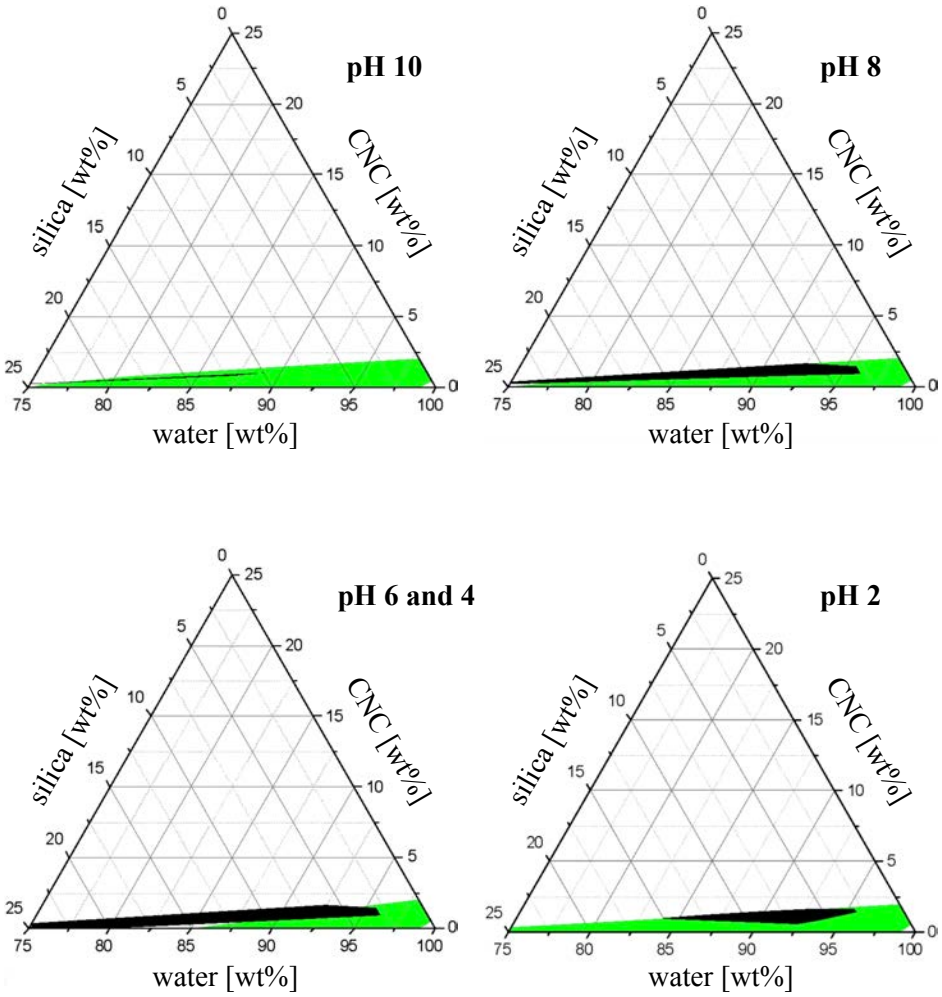

Figure 10. Ternary plots for silica/CNC mixtures at pH 10, 8, 6, 4 and 2. The green areas represents samples that have not gelled whereas the black areas represents samples that have gelled.

In the ternary plots in Figure 10 the gelling regions are black and the non-gelling regions are green. By studying the ternary plots the same gelling trends as for the scatter plots can be observed. The ternary plots also includes the water variable which gives a complete representation of the composition of the samples. While the individual samples are not shown in the ternary plots the gelling regions clearly show how the gelling regions change with changing pH. As have already been observed in the earlier plots the smallest gelling region occurs at pH 10 and the largest at pH 6 and 4.

These bulk gelling experiments gave a larger understanding in how silica and CNC gel; mostly in different mixtures but also individually. The synergy effect between CNC and silica was very noticeable.

4.2 Gelling in bath using syringe extrusion

After the gelling of the different mixtures of CNC and silica had been studied the focus was to study gelling in a coagulation bath using extrusion. These experiments were conducted to more closely resemble the spinning procedure that was the end goal of this project. The extrusion was performed by using a 2 ml syringe with a 0.8 mm needle. The syringe was then

filled with the CNC/ silica mixture that was then extruded at a slow rate into a gelling bath. The extrusion was done into both in small vials of 4 ml and into a gelling dish with a diameter of 7 cm.

Prior to the extrusion tests, the composition of the gelling bath had to be determined. Building on already acquired experimental data, one of the pHs (6 or 4) that resulted in the most samples gelling from the bulk gelling experiments was selected. Since there were two pHs (6 and 4) that resulted in an equal amount of gelling samples one of them had to be selected. The selected pH was pH 4.

Upon extruding the first samples it was discovered that the samples that had previously gelled in the bulk gelling experiments did not gel when being extruded into a gelling bath. One likely reason for this is that if a sample is extruded into a bath the gelling needs to be almost instant to avoid dissolution in the bath. This is because the volume of sample is very small compared to the volume of the bath. Even though the concentration in the sample is the same (as in the bulk gelling experiments) the surroundings and the gelling method has a very significant impact on the gelling of a sample. As has been discussed in the theory section, a higher salt concentration makes a silica sample gel faster at a pH around 6. The assumption was then made that a salt would have the same effect at a lower pH as well. $CaCl_2$ (calcium chloride) was selected as the salt to induce the gelling. They were gelled in a HCl bath containing $CaCl_2$. This bath was prepared by adding $CaCl_2$ to a solution containing HCl at pH 4. Worth noticing is that there is salt (sodium chloride) present in all the samples that contain silica as the silica is sodium stabilised. However, since this amount of NaCl was not enough to induce gelling for the CNC samples in the extrusion experiments, addition of $CaCl_2$ was necessary.

4.2.1 Syringe extrusion gelling in vials

At first the samples were extruded into small vials of 4 ml to study the gelling behaviour.

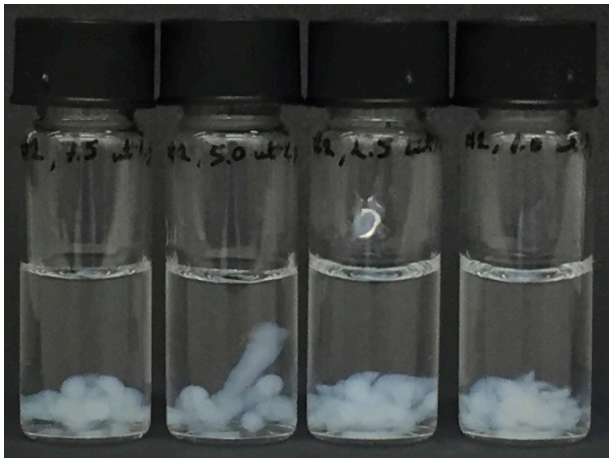

Figure 11. Extrusion gelling in 4 ml vials (2 ml liquid phase). Sample from left to right refers to sample 1-4 as described in Table 3.

Table 3. $CaCl_2$ concentrations for the corresponding vials in Figure 7.

Sample	1	2	3	4
$CaCl_2$ [wt%]	7.5	5.0	2.5	1.0

These samples (Figure 11, Table 3) show the gelling of a mixture of 9 wt% SiO_2 and 1.4 wt% CNC (on a dry basis 87 wt% silica/ 13 wt% CNC) in a bath with different concentrations of $CaCl_2$ at pH 4. These experiments were conducted to study the impact of the salt concentration on the gelling behaviour of a sample with this mixture of silica and CNC.

In Figure 7 from left to right the concentrations of $CaCl_2$ in the samples are: 7.5, 5.0, 2.5 and 1.0 wt%. When comparing the gelling effect of the different salt concentrations it was discovered that they were mostly similar. However, the 5 wt% $CaCl_2$ concentration gave the most stable gelling behaviour. This can be seen in vial 2 in Figure 7 where a longer fibre separated from the rest of the fibres can be observed on the wall of the vial. The gelling in this bath was instant with fibres that sunk to the bottom of the vial. The fibres were somewhat collectible but only in small pieces as they were very fragile. The same fragile behaviour would later be observed for all the samples that contained CNC and silica.

After deciding on using the 5 wt% $CaCl_2$ bath at pH 4 for gelling all further gelling experiments (using CNC) were conducted using gelling baths with this composition.

4.2.2 Gelling for pure CNC, 50 wt% CNC/50wt% silica and for pure silica

To examine the extrusion gelling properties of pure silica and pure CNC as well as a 50/50 mixture of the both three different sets of experiments were conducted. For these experiments 20 ml vials were used as they could simplify the extrusion process and the studying of the fibres.

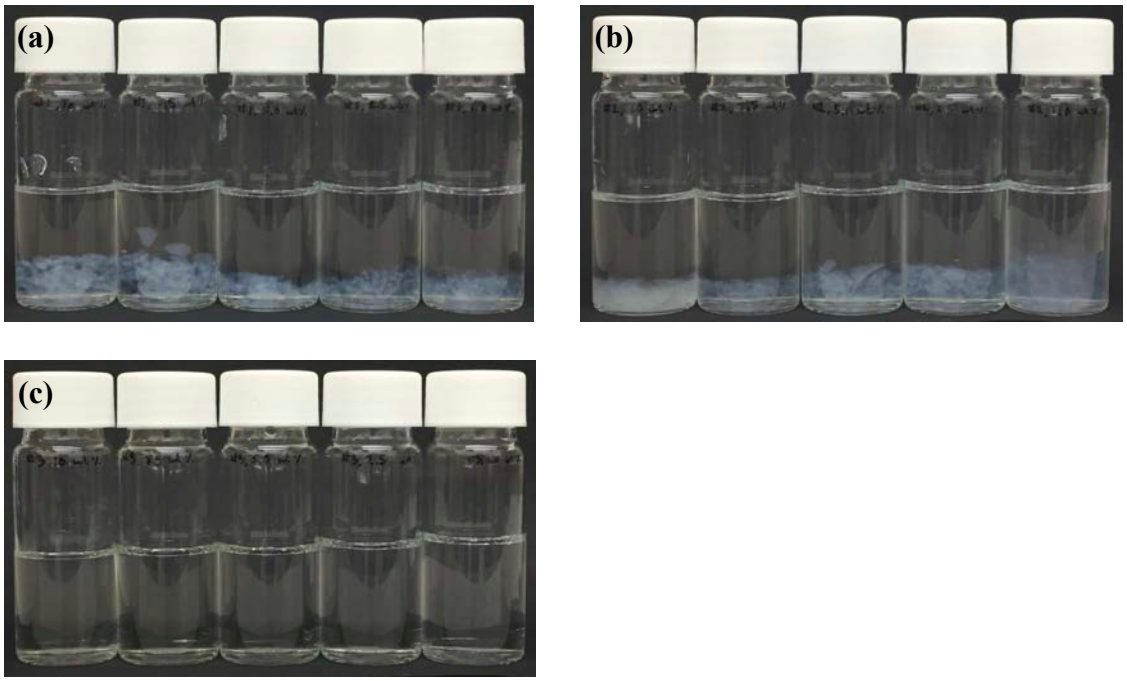

Figure 12: **(a)** 2 wt% CNC, **(b)** 2 wt% silica/2 wt% CNC and **(c)** 2 wt% silica.

In each of these sets of experiments the impact that five different concentrations of $CaCl_2$ could have on the gelling was examined. The amount of $CaCl_2$ in the baths varies in the same way for all the samples. From left to right the $CaCl_2$ concentrations are: 10, 7.5, 5.0, 2.5 and 1.0 wt%. When extruding the different samples into the vials clear differences could be observed between the samples.

Figure 12**(a)** shows that for the 2 wt% CNC the gelling at the different $CaCl_2$ concentrations was very similar. The most prominent gelling occurred in the samples with the highest $CaCl_2$ concentrations i.e. 10, 7.5 and 5.0 wt%. The vials with the 2.5 and the 1.0 wt% $CaCl_2$ displayed a significantly less prominent gelling than the other samples.

Figure 12**(b)** shows that for the 2 wt% silica/2 wt% CNC mixtures the same trend could be observed with decreased gelling for a decreased $CaCl_2$ concentration. For the samples with 2.5 and 1.0 wt% $CaCl_2$ the samples were more or less fully dissolved with fibres/gel that broke apart instantly upon touching them with a needle.

For the samples in Figure 12**(a)** and 12**(b)** it could be concluded that a $CaCl_2$ concentration above 5 wt% was necessary to get a decent gelling. For lower concentrations the gelling was so weak that the fibres could not be collected out of the gelling bath using a needle.

Finally, Figure 12**(c)** shows that for the pure 2 wt% silica there was no gelling. The mixture dissolved completely for all the different $CaCl_2$ concentrations leaving nothing to be collected and studied. This is an interesting observation as a pure CNC solution does gel as can be seen in Figure 12**(a)**.

Figure 13: Gelling at different $CaCl_2$ concentrations for 6 wt% silica and 1.6 wt% CNC (on a dry basis: 79 wt% SiO_2, 21 wt% CNC).

To further study the effect that $CaCl_2$ could have on gelling additional gelling experiments were conducted for 7.5, 5.0, 2.5 and 1.0 wt% $CaCl_2$. These samples are shown in Figure 13. The samples extruded into this gelling bath consisted of 6 wt% SiO2 and 1.6 wt% and the rest (92.4%) water. If the water is not considered the samples consist of 79 wt% silica and 21 wt% CNC. Once again, the coagulation bath with 5 wt% $CaCl_2$ displayed the best gelling properties with fibres gelling instantly and with sinking fibres that were somewhat collectible in small pieces.

To study the gelling and fibre forming properties more closely another type of gelling container was used. The container that was used was a dish with 7 cm diameter. For gelling in the dish a 50 ml 5 wt% $CaCl_2$ mixture was prepared by mixing $CaCl_2$ with HCl at
pH 4. By using this type of gelling container which is much wider it more closely approximates the gelling conditions of the final gelling container.

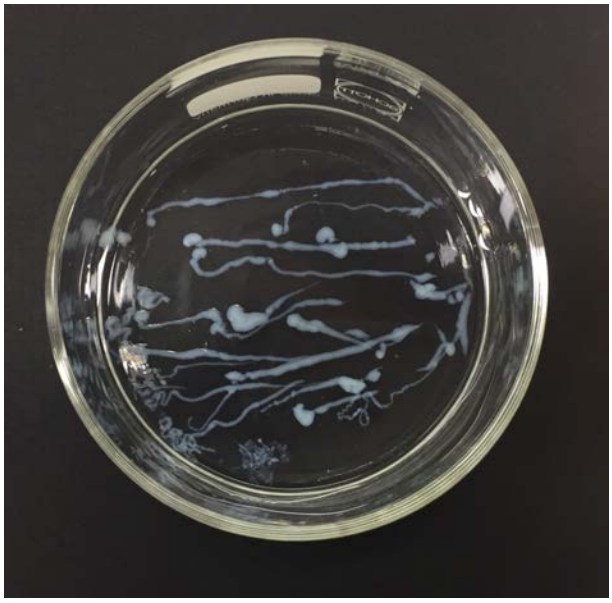

Figure 14: 10 wt% SiO_2/ 1 wt% CNC in 5 wt% $CaCl_2$ HCl mixture with pH 4. Dish diameter = 7 cm.

The use of a larger dish allowed longer fibres to be extruded. These fibres can be seen in Figure 14. It was also easier to have the fibres separated from each other and not stacked upon

each other as in the vials. The gelling in the dish was rapid and quite solid fibres were formed. These fibres were however, as before, quite stiff and brittle and broke relatively easily upon collection. The white/blue colour of the fibres occurred gradually within two seconds. As can be seen in the picture, the fibres are not of constant diameter and the thickness varies quite a bit between and within specific fibres. This was due to the inhomogeneity of the extrusion and the absence of a collection device.

To produce more fibres needed for the SEM analysis the gelling procedure was repeated for the following samples. For two of the samples CNF was used instead of CNC. The reason for this was to study possible material differences that the type of cellulose could have.

1. = 80 wt% SiO2 20 wt% CNC

2. = 50 wt% SiO2 50 wt% CNC

3. = 20 wt% SiO2 80 wt% CNC

4. = 80 wt% SiO2 20 wt% CNF

5. = 50 wt% SiO2 50 wt% CNF

6. = 20 wt% SiO2 80 wt% CNF

All of these samples (1 to 6) also had a non-calcined version to which the calcined samples could be compared.

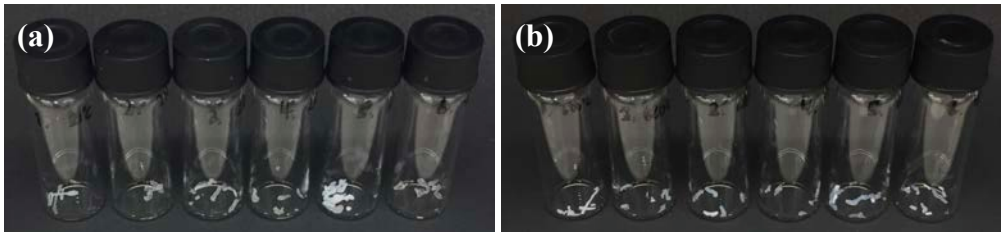

Figure 15: **(a)** Non-calcined samples and **(b)** calcined samples.

The non-calcined samples shown in Figure 15**(a)** were dried in room temperature on teflon plates. The calcined samples shown in Figure 15**(b)** were collected after being calcined for 4 hours at 600°C. They had mostly retained their shape except for the formation of few cracks. Most of the fibres stayed intact when being moved to the vials from the calcination beakers.

Figure 16: CNF fibres gelled in a HCl bath with pH 2. From left to right mixture extruded into the baths consists of 80, 70, 60 and 50 wt% CNF and 20, 30, 40 and 50 wt % silica). The wet fibres are visible above the level of liquid.

To examine the spinnability of the CNF fibres in larger vials with a pH 2 HCl solution four different vials, seen in Figure 16, were prepared. In contrast to CNC, the samples that contained CNF did not require any additional salt to induce the gelling. For these samples the gelling bath consisted of a HCl solution at pH 2. Fibres prepared from CNF instead of CNC are much more stable overall. This holds true even when varying the silica concentrations quite significantly. From left to right the different mixtures that were gelled were: 80, 70, 60 and 50 wt% CNF with the remaining percentages being silica. The observations for these samples were as follows:

80 wt%: Mostly lumps are formed but some fibres as well that are collectible and quite stable.
70 wt%: Not many lumps. Two long fibres are formed. These are collectible but quite brittle and breaks relatively easily upon collection.
60 wt%: Similar to 70 wt% but a few lumps are formed and a bit more brittle fibres.
50 wt%: Not many lumps. Even more brittle fibres that break somewhat upon collection.

4.3 Extrusion tests using a syringe pump

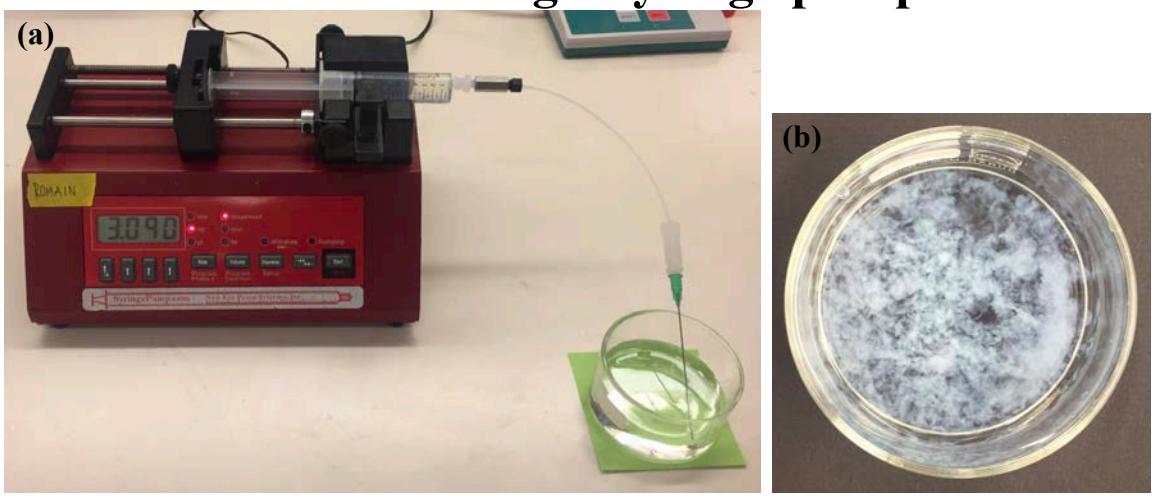

Figure 17: **(a)** Extrusion setup and **(b)** gelled fibres from extrusion setup in **(a)**.

To get closer to the setup that was going to be used for the spinning experiments at a larger scale the use of a syringe pump that would be used for those experiments was introduced. One benefit of this setup is to eliminate the variability inherent of extruding by hand. In this setup a syringe pump (Figure 17**(a)**) was used and set to extrude at a rate of 3 ml/min. This setup also allowed for the gelling of larger volumes, providing enough material for the nitrogen adsorption analysis. The same gelling bath as before was used in the syringe pump extrusion experiments.

After the silica/CNC (in this case) mixture had been gelled in the bath the gel had to be separated from liquid phase. As the mixtures that contained CNC were difficult to collect due to the fibres breaking apart and also due to the aforementioned necessity to collect larger masses of fibres a filtration system was set up for the separation (Appendix: "14 Collection using vacuum suction"). By using vacuum suction the fibres were separated form the coagulation/gelling medium and then collected for calcination to prepare them for the forthcoming nitrogen sorption analysis.

4.4 Fibre spinning

For spinning at a larger scale three different samples were selected. These can be seen in Table 3.

Table 3. Fibre mixtures for spinning of CNF fibres.

Sample	wt% SiO_2 (dry)	wt% CNF (dry)	m CNF (solution) [g]	m SiO_2 (solution) [g]	m (total) [g]	wt% CNF (sample)
1	79	21	12.07	7.95	20.02	0.2110
2	79	21	20.00	0.0933	20.09	0.3484
3	50	50	17.02	3.02	20.04	0.2973

In these experiments the extrusion was done through a needle with a diameter of 0.275 mm at an extrusion rate of 0.257 ml/min. The collection speed upon the collector was set to 3.5 m/min. For these experiments only mixtures that contained CNF were used. The reason for not using CNC was that in collecting the fibres upon the collector depicted below the strength of the fibres is required to be quite high for them to hold up under their own weight. This is because the fibres have to be much longer than in the gelling dish to be collected. In the gelling dish, fibres that used CNC were collectible but in very small pieces. For the nitrogen sorption analysis, the mass of collected fibres needed to be higher. Due to this the fibres had to be collected by using the vacuum suction setup. In using CNF in the same type of fibre spinning setup, the strength of the fibres was enough for them to be collected from the bath up on a collector. See Figure 18:

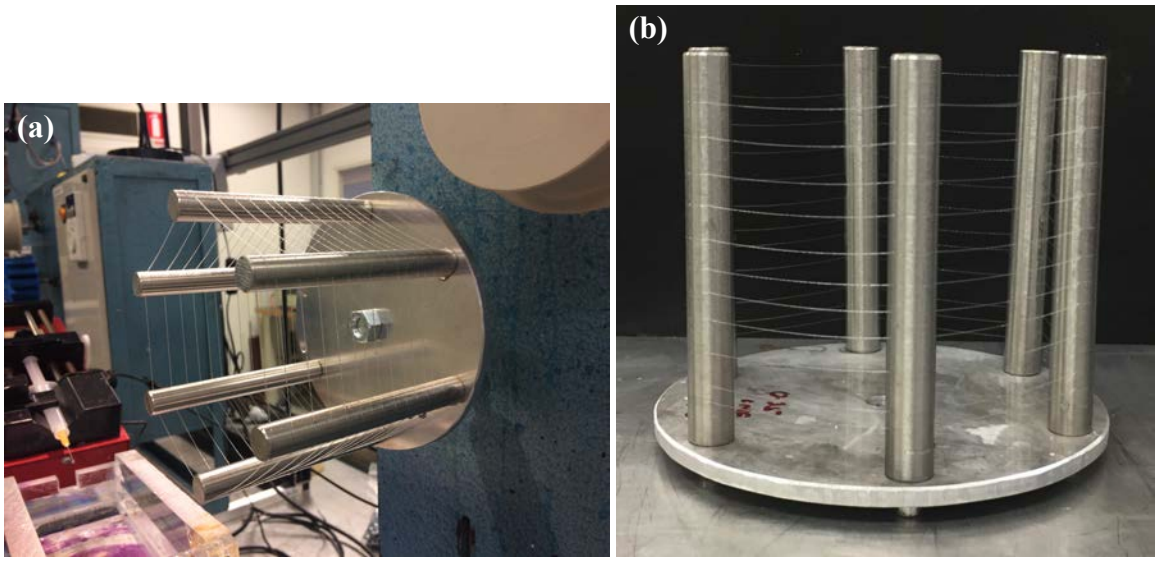

Figure 18: **(a)** A fibre spinning setup and **(b)** spun fibres of 79 wt% SiO_2, 21 wt% CNF (dried).

As can be seen in Figure 18**(b)** the fibres for sample 2 (79 wt% SiO_2, 21 wt% CNF) were intact after drying. This was not the case for the more diluted fibres (sample 1).
One important observation that can be made is that there was a dilution effect regarding CNF, i.e. the concentration of CNF in the samples is not the same. Sample 2 that had the same ratio of silica and CNC as sample 1 was not successful in forming fibres that could be collected and dried. The reason for this is attributed to that the concentration of CNF in sample 1 of 0.21% is much lower than the 0.35% concentration in sample 2. It has been shown that the amount of CNF in a mixture is crucial to its physical properties such as its collectability [34]. Further, it has also been shown that decreasing the concentration of nanocellulose in a suspension results in a change of the gelling behaviour of the suspension. Upon decreasing the nanocellulose concentration in a suspension a transition can be observed. In this transition the behaviour goes from behaving like a gel to behave like a liquid [34]. If a suspension that is too diluted is used, the wet strength of the fibre is not sufficient for it to be collected upon the collector [34].

4.5 SEM analysis of samples

Many of the samples that were produced were analysed using SEM. The results from these samples will now be presented and analysed.

There are a few different key aspects and comparisons that were the focus in the SEM analysis of these samples. Different types of areas and surfaces of the samples were examined. These are listed below.

1. Calcined and non-calcined samples
2. Cross sections and pristine surfaces. A pristine surface is a surface that was produced during the calcination and not a surface introduced post calcination due to breaking of the sample.
3. CNC and CNF samples
4. Crushed and intact fibres

It is important to remember that none of the fibres that had undergone calcination contain any CNC or CNF. They are, however referred to by the composition that they had prior to calcination to be able to tell them apart.

SEM analysis of intact fibres

Initially, two fibres that were analysed and compared were a non-calcined and a calcined fibre. They were compared to see if and in that case how the calcination had an effect on the outer surface of the fibre. Both fibres consisted of 79 wt% SiO_2 and 21 wt% CNC prior to calcination.

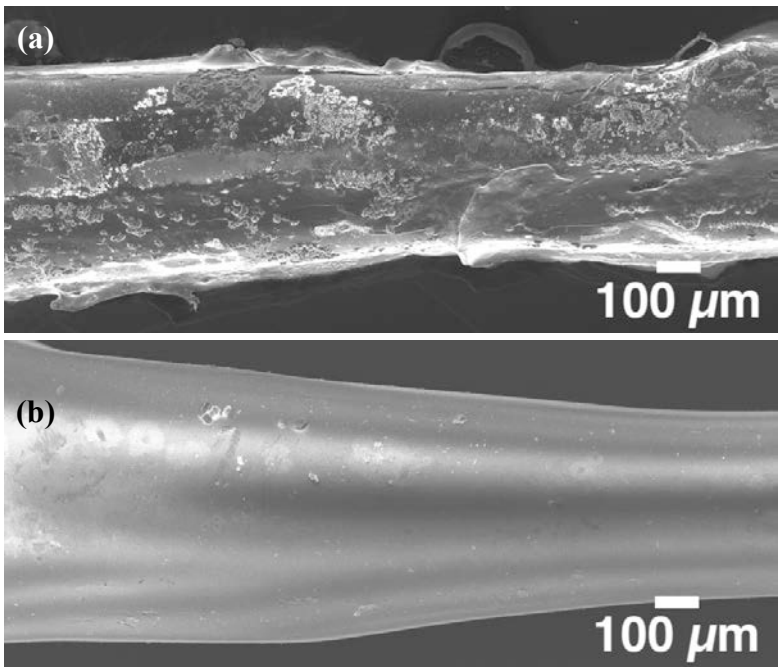

Figure 19: **(a)** Non-calcined fibre and **(b)**: calcined fibre.

From Figure 19**(a)** and **(b)** it can clearly be seen that the surfaces of the two samples are indeed different. The non-calcined fibre on the top has a very rough and non-uniform surface whereas the calcined fibre on the bottom has an almost perfectly smooth surface. The calcination has clearly had an effect on the surface of the fibre by removing the cellulose. Since the calcination process removes the CNC from the sample it is reasonable to assume that the roughness of the non-calcined sample was composed of CNC that was removed during calcination. It is also to be expected that some of the surface roughness of the non-calcined sample is due to it being covered was covered by salt ($CaCl_2$) used to induce the gelling.

Another observation is that none of the fibres have a consistent diameter. This is most likely due to the fact that the fibres were only extruded into a bath. When a fibre is spun, however, the fibre drawing increases the homogeneity. It does seem to be more consistent for the non-calcined fibre. However, in observing the diameter during collection of the fibres it could be seen that it varied quite a bit so no exact conclusions of the consistency of the diameter should

be drawn from the SEM. These SEM images are however useful to get an understanding of the range of diameters of the fibres.

SEM analysis of cross sections of CNC fibres

The next stage was to compare the cross sections of the same fibres to see if they had also been altered during the calcination. Again, the aim of the calcination was to remove the cellulose so that only the porous silica was left.

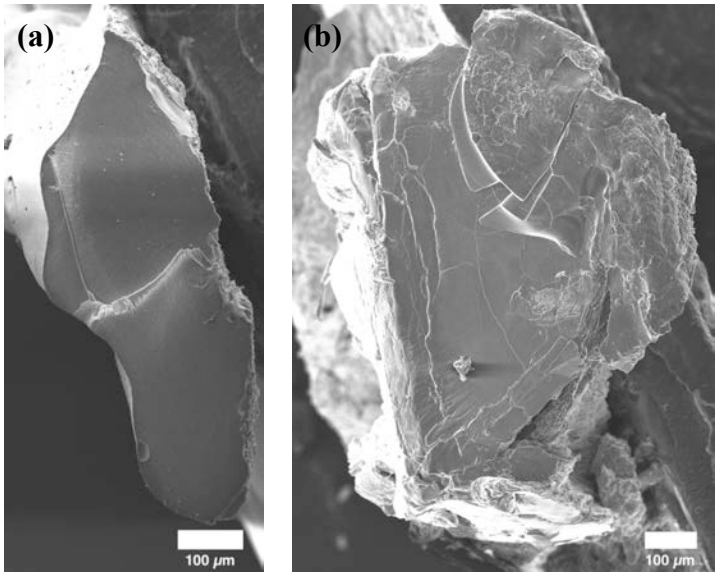

Figure 20: **(a)** Cross section non-calcinated sample and **(b)** cross section calcined sample.
(79 wt% Silica 21 wt% CNC)

In these first cross section SEM images it can be seen that the outer surface of the non-calcined sample (Figure 20 **(a)**) is much smoother than the surface of the calcined sample (Figure 20 **(b)**). The cross section is on this magnification scale smoother in the non-calcined sample with only a couple of different regions compared to numerous regions of different sizes and angles for the calcined sample.

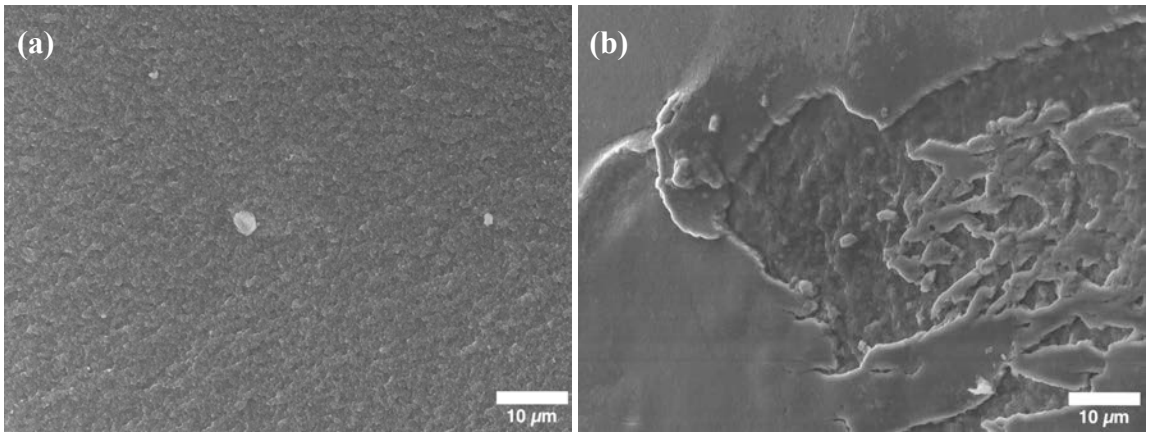

Figure 21: **(a)** Cross section non-calcined sample and **(b)** cross section calcined sample.
(79 wt% Silica 21 wt% CNC)

In studying the cross section of the material at higher magnification it can be seen that the non-calcined sample is more homogeneous with a continuous, somewhat rough, and seemingly porous structure. The calcined sample to the right has one quite even and one rougher section. The rougher section appears to have larger structures and pores than the non-calcined sample but this will be examined further at a higher magnification.

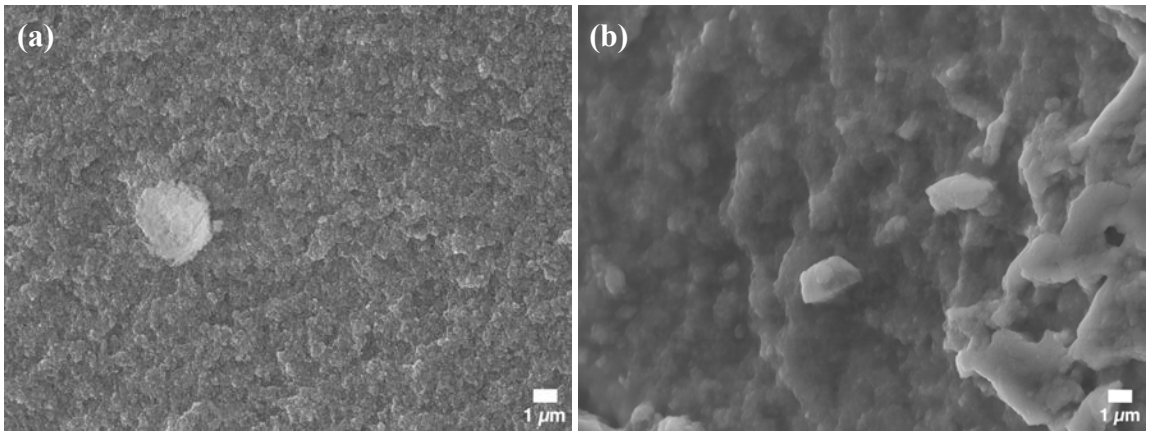

Figure 22: **(a)** Cross section non-calcined sample and **(b)** cross section calcined sample.
(79 wt% Silica 21 wt% CNC)

At 5000x magnification it can again be seen that the structure of the non-calcined sample is finer and with smaller pores than the calcined sample.

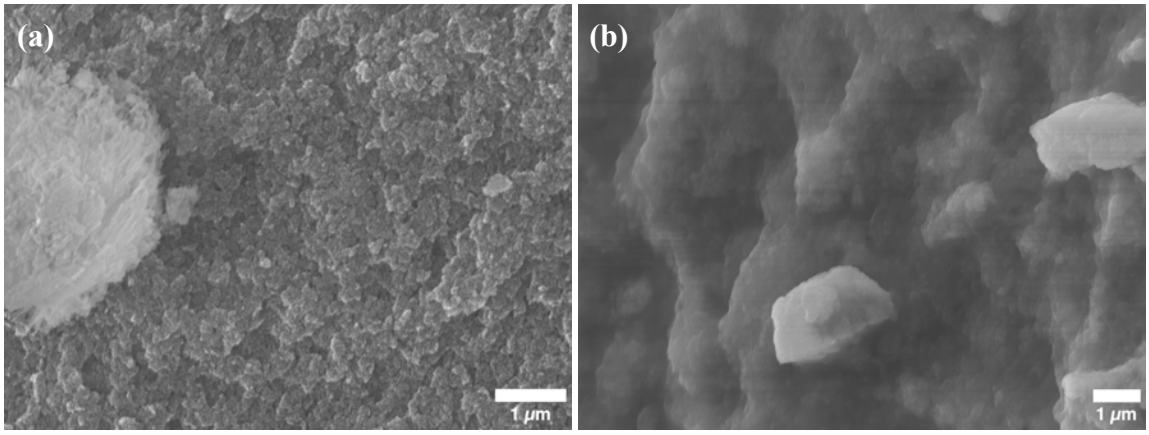

Figure 23: **(a)** Cross section non-calcined sample and **(b)** cross section calcined sample.
(79 wt% Silica 21 wt% CNC)

At 15000x magnification for the non-calcined sample and 10000x magnification for calcined sample the structure of the materials can be seen in closer detail and the difference in smoothness and pore size is even more evident. It is important to remember that even though the SEM images can give an indication of a porosity of a material nitrogen sorption analysis will be used to be able to quantify the porosity of the material.

Other fibres at different compositions were also studied. These SEM analyses were conducted to see if there were any differences in the structure between fibres of different CNC/silica concentrations.

First, the SEM analysis of the samples with silica and CNC will be presented and discussed. These samples are represented in Table 4.

Table 4: Silica/CNC concentrations of different mixtures.

Sample	SiO_2 [wt%]	CNC [wt%]
1	80	20
2	50	50
3	20	80

SEM analysis of CNC samples

It is interesting to compare the fibres before and after calcination. For this reason SEM was conducted for both non-calcined and calcined samples. However, after comparing the non-calcined and the calcined samples a clear trend (that will be discussed below) could be seen. Due to this only a few of the non-calcined SEM images are shown in this report but many additional SEM images can be found in Appendix “11 Additional SEM images”.

The first samples that were compared are the 80 wt% silica and 20 wt% CNC samples.

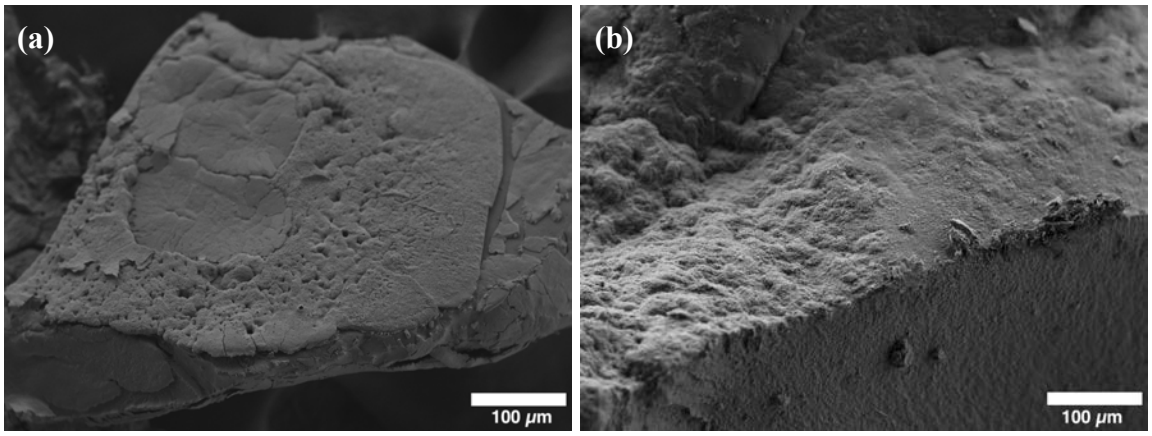

Figure 24: **(a)** Non-calcined sample and **(b)** calcined sample.
(80 wt% silica 20 wt% CNC)

These two first SEM images at 200x magnification shows two different pieces of the sample. The structure is smoother and less rough in the non-calcined sample. This is a difference that can be observed for all the samples. This smoothness is attributed to the non-calcined samples and their rough and porous structure being covered with cellulose.

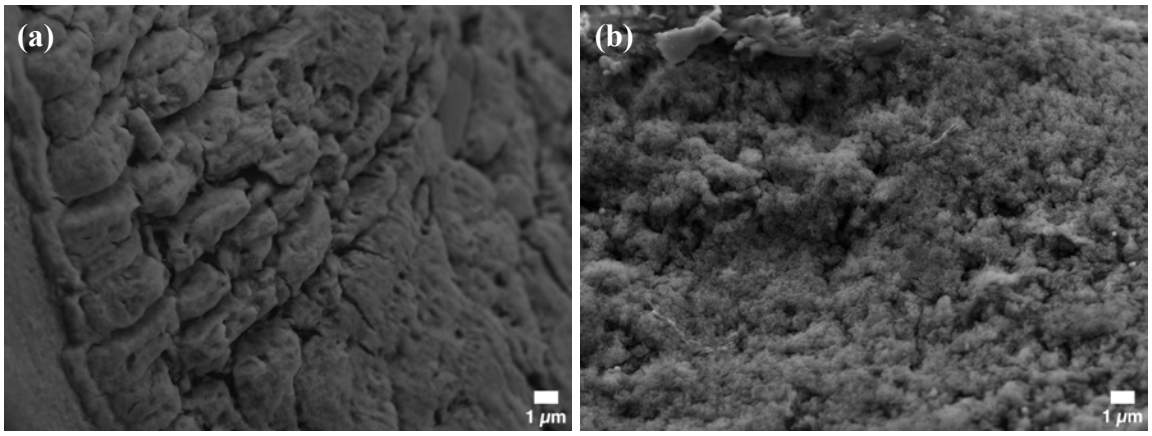

Figure 25: **(a)** Non-calcined sample and **(b)** calcined sample.

Studying the sample at 5000x magnification it is obvious that the structure of the calcined sample to the right is much more porous than the non-calcined structure. This is attributed to the CNC filling up and covering the pores that is formed by the silica structure.

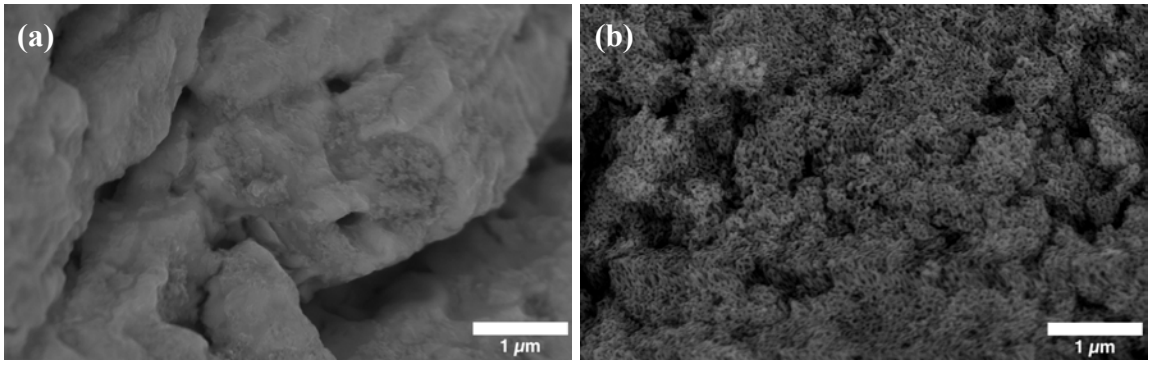

Figure 26: **(a)** Non-calcined sample and **(b)** calcined sample.

When comparing the non-calcined and the calcined samples at 20 000x magnification the small pores of the calcined sample are prominent throughout the sample. For the non-calcined sample the few pores present are much larger. One important observation is that the larger pores present in the non-calcined sample appears to be retained even after calcination. This means that the small pores are revealed during the calcination but not the larger pores and cracks of the material. From the SEM image the size of these smaller pores were estimated to be in between 20 and 40 nm. As the pore size is between 2 and 50 nm, this means that the material qualifies as being mesoporous. The significantly larger holes which are much more scarce, are around 0.5 μm in diameter. These larger holes should be considered irregularities. They are mostly present in the calcined sample but are, in contrast to the mesopores, also present in the sample prior to calcination.

It is important to remember that these measurements of the pore sizes and the given ranges of pore sizes are only rough estimations. They are based on SEM-images of a few μm^2 and should be only be viewed as rough comparisons between SEM images of samples of different silica/CNC ratios. For a quantitative estimation of the pore sizes and porosities of the different samples gas sorption experiments were also conducted and these results will be discussed later in the report.

As mentioned earlier, the final product should be calcined and therefore the focus is now switched to comparing samples of different CNC and silica content instead of comparing non-calcined and calcined samples.

4.6 Silica/ CNC at different ratios

The samples that will be compared now are the ones with 20, 50 and 80 wt% silica. The focus will be on comparing their structure and porosity at the surface of the fibre. To view the SEM images at other magnifications and the non-calcined samples for all of these, see Appendix: "11 Additional SEM images".

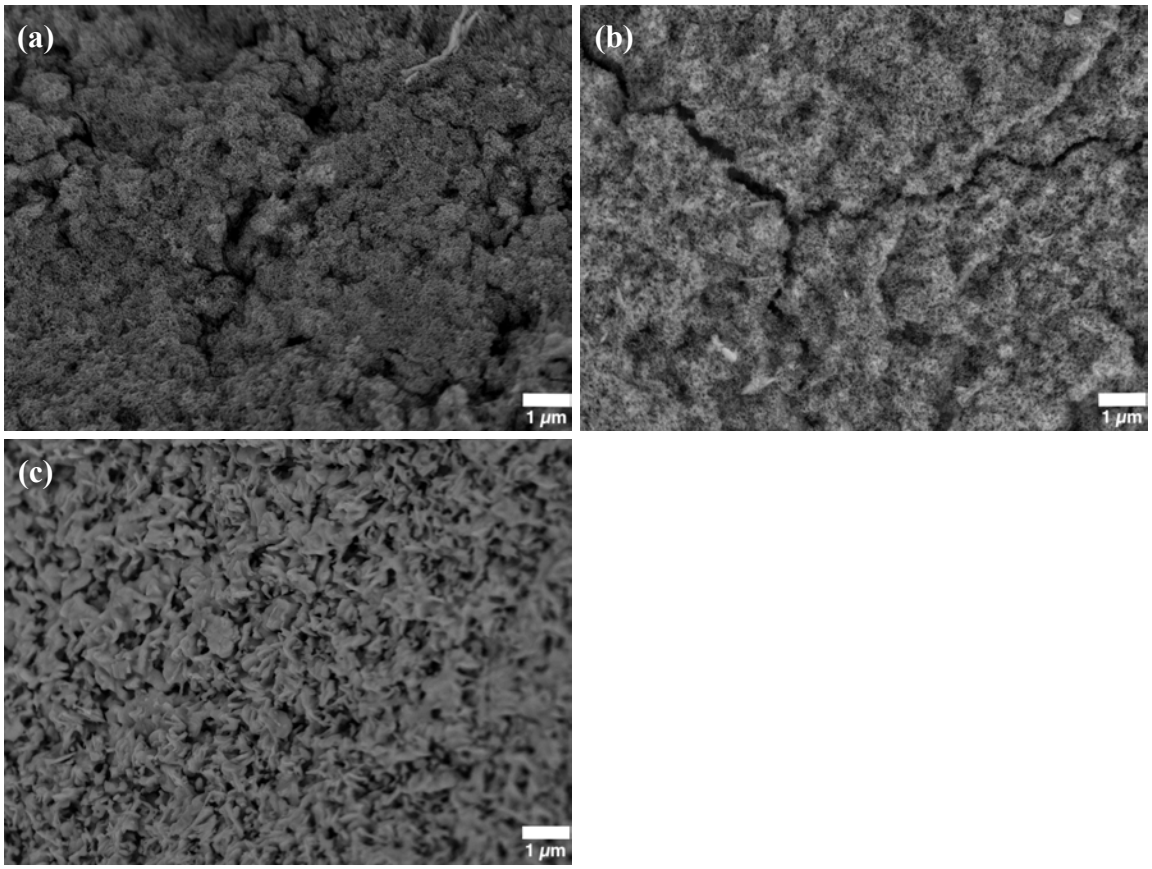

Figure 27: **(a)** 80 wt% SiO_2 20 wt% CNC, **(b)** 50 wt% SiO_2 50 wt% CNC and **(c)** 20 wt% SiO_2 80 wt% CNC. All samples are calcined.

When comparing the samples clear differences can be observed. One of these differences is that the pore size of the sample that initially had a 80 wt% CNC content (Figure 27**(a)**) is much larger than that of the sample with an initial CNC content of 50 wt% (Figure 27**(b)**). In measuring the pores from the SEM images it could be seen that the pore size for the sample with the lower initial CNC content ranged from 50 to 230 nm and for the higher CNC content it ranged from 90 to 380 nm. These are rough calculations from a small sections of SEM images. Due to this, to get quantifiable results, further analysis will be conducted using nitrogen sorption analysis. This will provide more more reliable comparisons between the different samples. The pore size of the 80 wt% silica 20 wt% CNC sample was discussed earlier and is between 20 and 40 nm. These findings are summarised in Table 5:

Table 5: Estimated pores sizes of different silica/CNC samples.

Sample	SiO_2 [wt%]	CNC [wt%]	pore size [nm]
1	80	20	20 - 40
2	50	50	50 - 230
3	20	80	90 - 380

An obvious finding when comparing the pore sizes of these different samples is that the pore size increases with increasing initial CNC concentration. This is not that surprising as the CNC can prevent the silica clusters from interacting more closely. Therefore, an increase in CNC concentration of the collected fibres is likely to lead to a less packed network of silica nanoparticles and an increase in porosity after calcination. This is due to the fact that the CNC is removed during calcination leaving only the silica.

4.7 SEM of spun CNF fibres

The CNF fibres collected on the collector in the large-scale spinning were analysed using SEM. The analysis was conducted using both a backscattered electron detector (BED) and and a lower electron detector (LED).

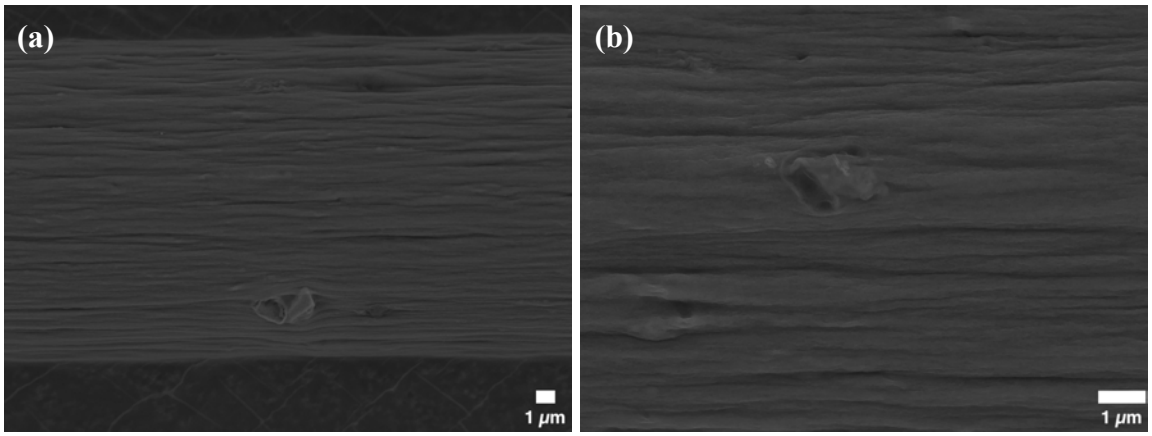

Figure 28: **(a)** CNF fibre (4000x) and **(b)** intact CNF fibre (10 000x). Both fibres are non-calcined.
(80 wt% Silica 20 wt% CNF)

In these SEM images it can clearly be seen how the fibres are intact without any cracks and with a smooth outer surface. The surface has few visible impurities and are very homogenous.

The diameter of the fibre was approximated to 16.8 µm and remain constant throughout the fibre. The cross section of the fibre with 80 wt% silica and 20 wt% CNF was analysed using SEM but also with EDS (Energy-dispersive X-ray spectroscopy) to determine the chemical composition of the sample.

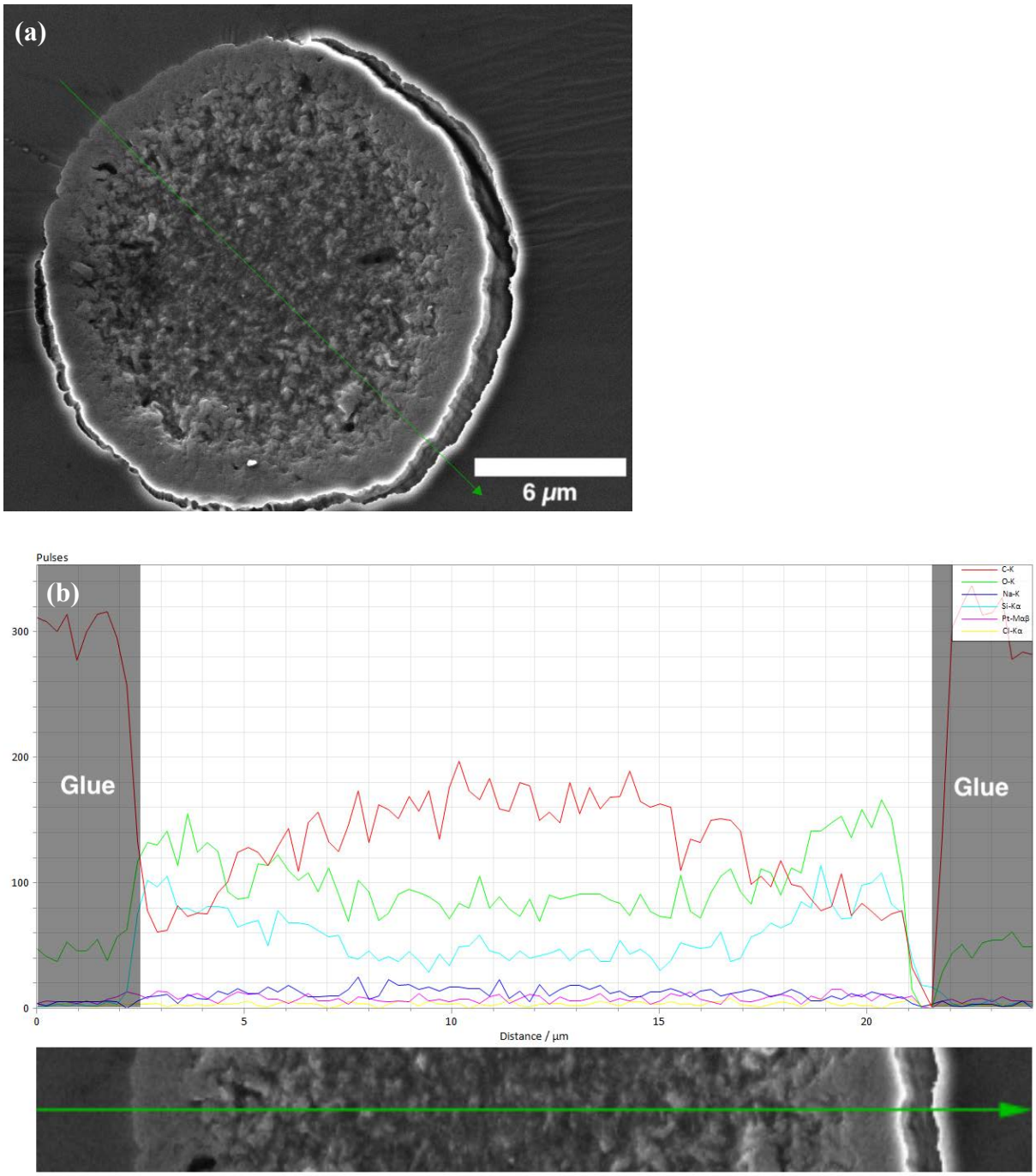

Figure 29: **(a)** Cross section of a CNF fibre (80 wt% silica and 20 wt%) and **(b)** EDS of the cross-section. The outer less porous region of the sample is the epoxy (glue) in which the fibre is imbedded. (80 wt% silica and 20 wt% CNF)

It can be seen in Figure 29**(a)** that the fibre appears to have a quite rough structure. This rough structure is likely a porous part of the fibre that is covered up by CNF. This rough part is surrounded by a more dense part. This outer surface is the glue in which the fibre is embedded.

In studying the EDS for the cross section several interesting conclusions can be drawn. The first is that the sample is composed of approximately 20% carbon. This correlates well to the the silica/CNF mixture prior to gelling (CNF is the source of the carbon).

Studying the EDS of the cross-section of the fibre it is evident that the Si/C ratio is not constant. From the edge of the fibre towards the centre it can be seen that the carbon content increases as the silica content decreases. This composition profile is symmetrical and this underscores the influence that the spinning process has on the composition of the fibre. It can be explained by the shear forces in the spinneret that introduces a variation in the composition between the centre and the the sides of the fibres.

4.8 Nitrogen sorption analysis

To determine the surface area, pore volume and pore size of the silica nitrogen sorption analysis using the nitrogen sorption analysis method was used. The reason for selecting these samples were that many of them had already been analysed using SEM. Additionally, a comparison between crushed and intact fibres was conducted, fibres calcined at different temperatures and CNF fibres. There were nine different samples that were analysed using this method. These are listed in Table 6.

Table 6: Silica/CNC and Silica/CNF samples for nitrogen sorption analysis. Note that these samples have all been calcined prior to measurements so the CNC content is that prior to calcination.

Sample	**wt% SiO_2**	**wt% nano-cellulose**	**Additional information**	**Nitrogen sorption surface area [m^2/g]**	**Pore volume [cm^3/g] (BJH Adsorption average)**	**Pore size [Å] (adsorption average pore width)**
1	80	20	Intact	62.3155	3.606910	87.4397
2	50	50	Intact	24.8739	0.153003	125.9920
3	20	80	Intact	12.3137	0.165265	162.8129
4	80	20	Crushed	64.2907	0.238710	123.4116
5	50	50	Crushed	27.1324	0.242086	189.0492
6	20	80	Crushed	13.0296	0.239495	38.4061
7	50	50	8 hours	44.7440	0.227296	135.6171
8	50	50	700°C	3.3945	0.059767	251.9817
9	79	21	CNF	204.8140	0.535634	88.7834
Reference	100	0	Pure SiO_2	122.6742	0.410517	131.3304

The data from Table 6 can also be represented in a plot as in Figure 30:

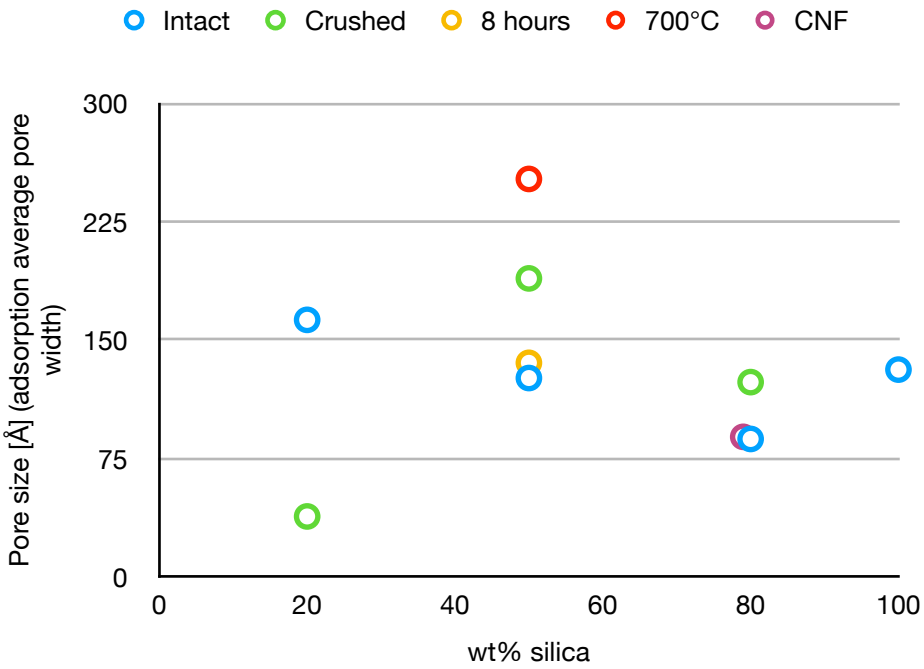

Figure 30: Pore size of the samples from the nitrogen sorption analysis.

4.9 Effect of the sample texture

Sample 1-3 were crushed and analysed again to determine whether their relative large pieces had an influence on the pore size.

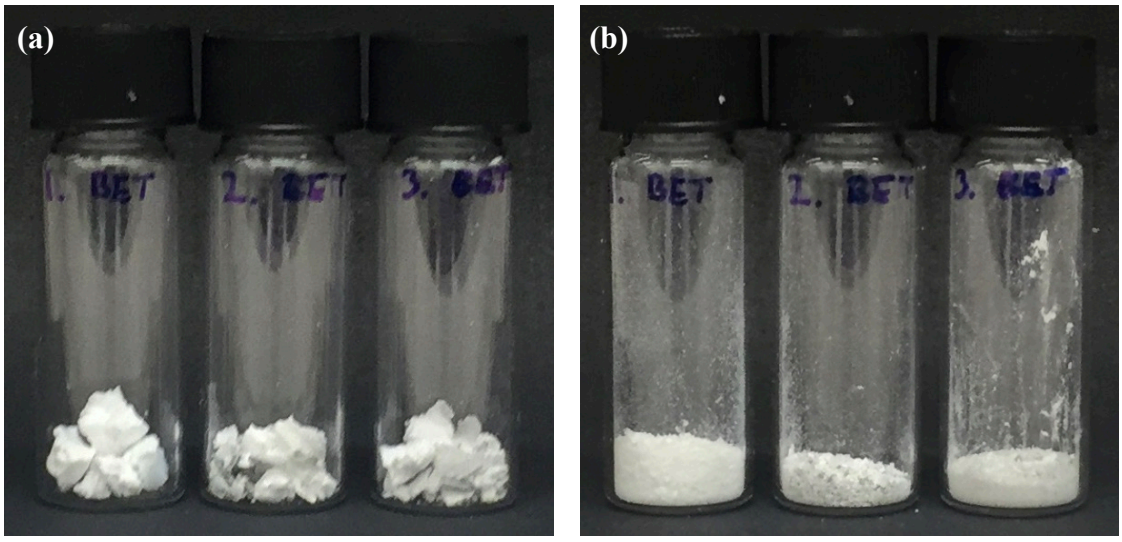

Figure 31: **(a)** Sample 1-3 (intact) and **(b)** sample 4-6 (crushed). This figure shows how the macrostructure changed after the samples had been crushed.

A hypothesis prior to further analysis was that the pores may have been restricted from the outer surface due to a collapse of the pores during calcination. However, the surface area only increased a few percent between the samples. More specifically the surface area increased with 3.2% for the sample with 80 wt% SiO_2, 9.1% for the sample with 50% SiO_2 and with 5.8% for the sample with 20 wt% SiO_2. Due to these findings the increase in surface area can

more likely be attributed to the fact that the outer surface area increases if a material is broken into smaller pieces. If it was the case that the breaking of the pieces indeed had an effect on increasing the accessibility to pores hidden within the material a more significant difference between the samples would have been observed. Considering this the crushed samples (sample 4-6) will not be discussed further as they are very similar to their intact versions.

When considering the pore size (adsorption average pore width) of the samples before and after being crushed another trend could be observed. Now the pore size increased with 41% for the sample with 80 wt% silica and with 50% for the sample with 50 wt% silica. For the sample that initially had 20 wt% silica and 80 wt% CNC, however, the pore size has decreased dramatically (76%) after the crushing. This may be due to this sample being much softer than the other two and the crushing of it required much less energy. This resulted in it breaking into smaller pieces upon being crushed. This may also more or less have led to the collapsing of the pore structure that was initially present in the material.

For sample 1 and 2 the more robust structure of the material and the pores may explain why the pore size did not decrease upon crushing the samples. An explanation to the increase in pore size may be that some pores had collapsed and formed larger ones.

4.10 Effect of calcination temperature

Heating to 700° had a profound impact on the properties of the sample. First of all, the surface area decreased dramatically from 24.9 m^2/g for a sample with the same composition at 600°C to 3.39 m^2/g at 700°C. It is therefore evident that calcination at 700°C is not recommended if the target material should be porous. The pore size doubled from 126 to 252 Å after calcination. However, even if the pore size is now twice as large it does not take away from the fact that the presence of pores altogether has changed so dramatically. The pores that are present may be twice as large but they are barely existing in comparison to the amount of pores present when calcinating at 600°C.

Figure 32 shows the impact on the structure by calcinating at 700°C.

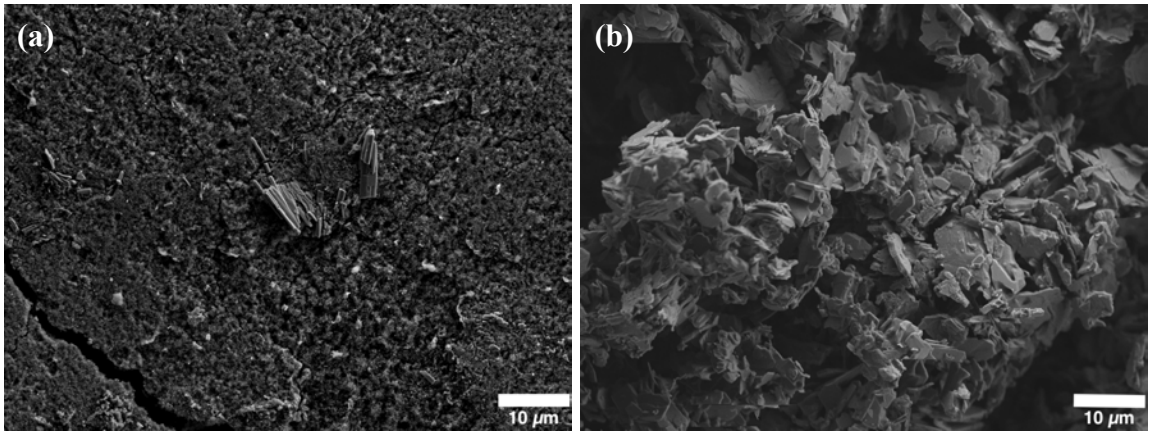

Figure 32: **(a)** Sample calcined at 600°C and **(b)** sample calcined at 700°C.

By studying these two SEM images it is once again evident that calcinating at 700°C significantly alters the structure of the silica and makes the material unusable for the targeted applications. The reason for this is that the material has broken into small pieces that according to adsorption analysis have a very low porosity.

4.11 Effect of calcination duration

It was also of interest to study how and if the duration of the calcination had an impact on the surface area, pore volume and pore size of the silica. To study this, a sample was calcined at 600°C for 8 hours instead of 4. When comparing sample two and sample seven which both consisted of 50 wt% silica and 50 wt% CNC prior to calcination a few changes could be observed. In comparing the surface area between the two samples it could be seen that it had increased from 24.9 m^2/g (4 hours) to 44.7 m^2/g (8 hours). This is a very interesting finding and it may very well be that a longer calcination would increase the porosity for the other samples as well. Further studies would have to be conducted to see if this finding would indeed hold true for other samples as well.

In regards to the pore width it could be seen that it increased slightly from 126 Å to 136 Å by calcinating for 4 hours longer. In comparison to the change in surface area the impact that a longer calcination time had on the pore size of the silica was much less prominent.

The SEM images in Figure 33 shows one 50/50 sample calcined at 600°C for 4 hours and the other a sample of the same composition calcined for at 600°C for 8 hours.

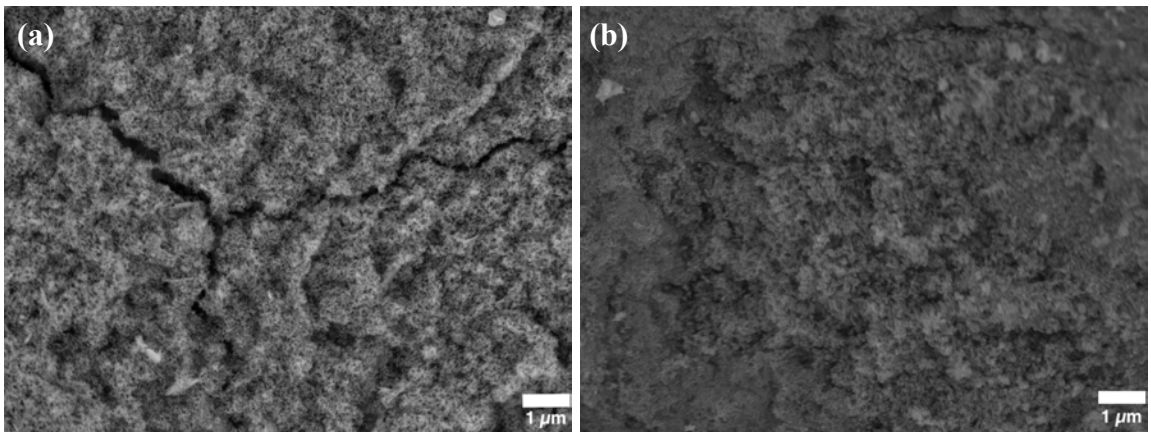

Figure 33: **(a)** Sample calcined for 4 hours and **(b)** sample calcined for 8 hours.
(50 wt% SiO2/50 wt% CNC)

In just studying these two SEM images (Figure 33**)** no clear differences in porosity can be observed. A crack is present in the sample that was calcined for a shorter time (Figure 33**(a)**) but this is attributed to a local defect of that sample and cracks like these are likely present even with a longer calcination time.

4.12 Effect of initial CNC content

The impact on the porosity of the final calcined silica in relation to its initial CNC content is important to consider. In this project the CNC has been used as a means of collection the samples after being gelled in a bath; either by aiding in the gelling, by forming a fibre that can easily be collected or both.

The surface area of the final silica is inversely correlated to the amount of CNC in the mixture prior to calcination. When increasing the amount of CNC in the sample from 20 to 50 wt% a dramatic decrease of the porosity can be observed. The porosity difference between the two mixtures is 60%. The difference in porosity between sample 2 and 3 (50 and 80 wt% CNC) is 50 wt%.

5 Conclusions

The main aim of this project was to study if it was possible to produce mesoporous silica through a spinning process.

To understand how different mixtures of silica and nanocellulose gelled at different pHs (pH 2, 4, 6 and 10) bulk gelling experiments were conducted. In these, the pH of different mixtures was lowered using HCl and the presence of gelling was determined using the inverted test tube technique. From these experiments it could be concluded that there was a clear synergy effect between CNC and silica. e.g. by mixing 3-15 wt% silica with 0.6-1.6 wt% CNC gelling could be induced at pH 2-8. Pure silica or CNC mixtures at these concentrations do not gel by themselves. It could also be seen that pure 30 wt% bare colloidal silica gels at a pH of 4 to 10. At pH of 4 and 6 pure silica also gels at silica concentration as low as 20 wt%. Finally, it was concluded that pure CNC in concentrations between 0.5 and 2 wt% does not gel for any pH between 2 and 10.

It was evident that also the pH of a mixture of silica and CNC had a significant impact on the gelling. Out of pHs 2, 4, 6, 8 and 10 the largest amount of samples gelled at pH 4 and 6 (equal number of samples at pH 4 and 6) followed by pH 8. This means that there was an optimum for the pH over and below which fewer samples gelled.

To get closer to approximating a spinning process syringe extrusion experiments were conducted. In these, different mixtures of CNC and silica were extruded into a bath with pH 4. Initially, there was no gelling but experiments showed that using the salt $CaCl_2$ at 5 wt% in the bath was the most efficient way to induce gelling in these mixtures. It was concluded that fibres formed using CNC and silica were quite fragile even when salt induced gelling was introduced. This was true for a 50/50 mixture of 2 wt% CNC and 2 wt% silica as well as a 21 wt% CNC/79 wt% silica mixture. This means that CNC was not a suitable agent for fibre spinning at this stage.

Even if fibres produced using CNC were not suitable for fibre spinning studying their structure was still of interest. This was done using SEM. In comparing a non-calcined and a calcined sample of 79/21 wt% silica/CNC it was evident that the surface of the non-calcined sample was covered up by cellulose. When the cellulose was removed using calcination a mesoporous structure was reviled.

Experiments conducted where the CNC content in a CNC/silica mixture was increased lead to an increase in pore size of the final calcined silica. This was attributed to the CNC preventing the silica particles from interacting more closely.

It was evident that by using CNF instead of CNC much tougher fibres could be produced. These fibres were stable and could be collected either using spinning or by collecting them directly from a gelling bath. For these, fibre mixtures of 79 wt% silica and 21 wt% CNF could be spun in larger scale. These fibres were intact even after drying in room temperature.

To analyse the porosity of the produced materials nitrogen adsorption analysis was conducted. This analysis showed that the silica that was mixed with CNC did not produce very porous silica fibres after calcination. The porosity for the samples were between 12 and 62 m^2/g for intact fibres and between 13 and 64 m^2/for crushed fibres. This indicates that CNC is not a viable template for producing porous silica. However, by using CNF a much more porous silica could be produced with a surface area of 205 m^2/g after calcination. These values should be compared to the surface area of pure silica oven dried silica which is 123 m^2/g.

Since mixtures of silica and CNF (79/21) could be spun at a large scale and CNF was shown to produce porous fibres it can be concluded that using CNF as a template to spin fibres of mesoporous silica shows promise.

6 Future work

There are several additional experiments that could have been explored during this master's thesis but restrictions, stated under "Limitations" in the beginning of the report, had to be made.

When considering the results of this project and the conclusions made in the previous section a few recommendations for further possible work will now be made.

Mixtures of up to about 79 wt% silica and 21 wt% CNF showed excellent spinnability. Further experiments to examine even higher silica contents and their impact on the spinnability would be very interesting to conduct. Experiments such as these could show at which silica/CNF ratio the fibres become difficult to collect using the wet spinning method described in this thesis.

Using salt free non-sodium stabilised (ion-exchanged) silica instead of the sodium stabilised silica for the gelling experiments to examine whether the (relatively low) salt content of the silica has an impact on the gelling.

CNF fibres did not gel without introducing the presence of $CaCl_2$ in the gelling bath. By examining another salt as well, preferably NaCl, the ability of the two salts to induce gelling could be compared.

In this project one type of silica Levasil CS30-236 was used. Further experiments using other types of colloidal silica with other particle sizes could be used to show how and if the size of the particles influence the porosity of the final silica material.

As the CNF/silica fibres showed great promise in producing highly mesoporous silica fibres after calcination, further experiments with CNF should be conducted. E.g. CNFs of different concentrations could be explored and experiments that tested their relative ability to form stable fibres with different amounts of silica could be studied.

It would also be interesting to study the physical properties of the fibres in closer detail using rheology. This would give a more thorough picture regarding the gelling behaviour of the mixtures whereas the inverted test tube technique only provides a binary description of the gelling. Using rheology, the properties of different fibres could be compared and enabling for the selection of the most suitable fibres to be used for spinning experiments.

7 References

[1] Carter, C. Barry, and M. Grant Norton. Ceramic materials: science and engineering. Vol. 716. New York: springer, 2007.

[2] Liou, Tzong-Horng, and Chun-Chen Yang. "Synthesis and surface characteristics of nanosilica produced from alkali-extracted rice husk ash." Materials science and engineering: B 176.7 (2011): 521-529.

[3] Nandiyanto, Asep Bayu Dani, et al. "Synthesis of spherical mesoporous silica nanoparticles with nanometer-size controllable pores and outer diameters." Microporous and Mesoporous Materials 120.3 (2009): 447-453.

[4] Johnson, Stacy A., Patricia J. Ollivier, and Thomas E. Mallouk. "Ordered mesoporous polymers of tunable pore size from colloidal silica templates." Science 283.5404 (1999): 963-965.

[5] Gustafsson, Hanna. Enzyme immobilization in mesoporous silica. Chalmers University of Technology, 2013.

[6] Trewyn, Brian G., et al. "Biocompatible mesoporous silica nanoparticles with different morphologies for animal cell membrane penetration." Chemical Engineering Journal 137.1 (2008): 23-29.

[7] Gallis, Karl W., et al. "The Use of Mesoporous Silica in Liquid Chromatography." Studies in Surface Science and Catalysis. Vol. 129. Elsevier, 2000. 747-755.

[8] áDe Stefanis, A. "Mesoporous M41S materials in capillary gas chromatography." Chemical Communications 15 (1997): 1343-1344.

[9] Jedvert, Kerstin, and Thomas Heinze. "Cellulose modification and shaping–a review." Journal of Polymer Engineering 37.9 (2017): 845-860.

[10] Dumitriu, Severian, Pierre F. Vidal, and Esteban Chornet. "Hydrogels based on polysaccharides." Polysaccharides in medicinal applications (1996): 87-105.

[11] Tashiro, Kohji, and Masamichi Kobayashi. "Theoretical evaluation of three-dimensional elastic constants of native and regenerated celluloses: role of hydrogen bonds." Polymer 32.8 (1991): 1516-1526.

[12] Rojas, Orlando J., ed. Cellulose chemistry and properties: fibers, nanocelluloses and advanced materials. Vol. 271. Springer, 2016.

[13] Nechyporchuk, Oleksandr, Mohamed Naceur Belgacem, and Julien Bras. "Production of cellulose nanofibrils: A review of recent advances." Industrial Crops and Products 93 (2016): 2-25.

[14] Hasani, Merima. Chemical modification of cellulose-new possibilities of some classical routes. Chalmers University of Technology, 2010.

[15] Oguzlu, Hale, Christophe Danumah, and Yaman Boluk. "Colloidal behavior of aqueous cellulose nanocrystal suspensions." Current Opinion in Colloid & Interface Science 29 (2017): 46-56.

[16] Cranston, Emily D., and Derek G. Gray. "Morphological and optical characterization of polyelectrolyte multilayers incorporating nanocrystalline cellulose." Biomacromolecules 7.9 (2006): 2522-2530.

[17] Lawrence, X. Yu. "Pharmaceutical quality by design: product and process development, understanding, and control." Pharmaceutical research 25.4 (2008): 781-791.

[18] Bordes, Romain, and Theo GM van de Ven. "Nanocellulose: What used to be cellulose micelles." Current Opinion in Colloid & Interface Science 100.29 (2017): A1-A2.

[19] Simonsson, Isabelle, et al. "The specific co-ion effect on gelling and surface charging of silica nanoparticles: Speculation or reality?." Colloids and Surfaces A: Physicochemical and Engineering Aspects 559 (2018): 334-341.

[20] Iler, Ralph K., and R. Iler. "The chemistry of silica: solubility, polymerization, colloid and surface properties, and biochemistry." (1979).

[21] Chapel, J-P. "Electrolyte species dependent hydration forces between silica surfaces." Langmuir 10.11 (1994): 4237-4243.

[22] Johnsson, Ann-Cathrin JH, M. Caterina Camerani, and Zareen Abbas. "Combined electrospray-SMPS and SR-SAXS investigation of colloidal silica aggregation. Part I. Influence of starting material on gel morphology." The Journal of Physical Chemistry B 115.5 (2011): 765-775.

[23] Gong, Tian, et al. "Gelation of hydroxyethyl cellulose aqueous solution induced by addition of colloidal silica nanoparticles." International journal of biological macromolecules 134 (2019): 547-556.

[24] Daniel-da-Silva, A. L., et al. "Rheological behavior of thermoreversible κ-carrageenan/ nanosilica gels." Journal of colloid and interface science 320.2 (2008): 575-581.

[25] Lundahl, Meri J., et al. "Spinning of cellulose nanofibrils into filaments: a review." Industrial & Engineering Chemistry Research 56.1 (2017): 8-19.

[26] Greiner, Andreas, and Joachim H. Wendorff. "Electrospinning: a fascinating method for the preparation of ultrathin fibers." Angewandte Chemie International Edition 46.30 (2007): 5670-5703.

[27] Voigtländer, Bert. Atomic Force Microscopy Second Edition. Springer, Cham, 2019.

[28] Goodhew, Peter J., and John Humphreys. Electron microscopy and analysis. CRC Press, 2000.

[29] Reimer, Ludwig. Scanning electron microscopy: physics of image formation and microanalysis. Vol. 45. Springer, 2013.

[30] Goldstein, Joseph I., et al. Scanning electron microscopy and X-ray microanalysis. Springer, 2017.

[31] Osaki, Toshihiko. "Effect of sol–gel conditions on BET surface area, pore volume, mean pore radius, palladium dispersion, palladium particle size, and catalytic CO oxidation activity of Pd/Al 2 O 3 cryogels." Journal of Porous Materials 25.3 (2018): 697-711.

[32] Naderi, Majid. "Surface Area: Brunauer–Emmett–Teller (BET)." Progress in filtration and separation. Academic Press, 2015. 585-608.

[33] Tanaka, Joh. "Evaluation of gel point." Gels Handbook. Academic Press, 2001. 51-64.

[34] Nechyporchuk, Oleksandr, et al. "Continuous assembly of cellulose nanofibrils and nanocrystals into strong macrofibers through microfluidic spinning." Advanced Materials Technologies 4.2 (2019): 1800557.

Appendix

1 Preparation of CNC solutions

Two samples of 1 and 2 wt% CNC were prepared using Milli-Q water and CNC (Levasil CS30-236) from Akzo Nobel. The samples were set to stir for 24 hours using a RCT basic magnetic stirrer form Kika labortechnik at 500 rpm in room temperature to fully dissolve the CNC. The CNC was then transferred to a different beaker and sonicated for 5 minutes three times using a Sonics Vibra Cell. This was done to homogenise the sample. Prior the homogenisation the sensor tip was cleaned using distilled water. The sample was the transferred back to the flask.

Preparation of different CNC/silica mixtures

Table A.1: Composition of a series of CNC/silica samples.

Silica	wt% SiO2	wt% SiO2 sample		CNC	wt% CNC	wt% CNC sample
0	30	0		2	0,5	0,5
0,2	30	3		1,8	0,5	0,45
0,4	30	6		1,6	0,5	0,4
0,6	30	9		1,4	0,5	0,35
0,8	30	12		1,2	0,5	0,3
1	30	15		1	0,5	0,25
1,2	30	18		0,8	0,5	0,2
1,4	30	21		0,6	0,5	0,15
1,6	30	24		0,4	0,5	0,1
1,8	30	27		0,2	0,5	0,05
2	30	30		0	0,5	0

These 11 different samples is one complete series that would be used for the studying of the gelling behaviour of individual samples after lowering the pH to a specific value.

11 new samples were prepared using the 1 wt% CNC. They were mixed with silica in the same manner as with the 0.5 wt% CNC.

For these samples the target pH was 8.

Table A.2: pH adjustment with HCl for a series of CNC/silica samples.

Sample	Inital pH	pH (Added HCl [µl])	Total volume HCl added [µl]
1	7.3	7.1 (no addition)	0
2	10.5	1.2 (200)	200
3	10.6	10 (20), 8.3 (50), 7 (10)	80
4	10.6	9.1 (60), 8.8 (10), 8.4 (10), 8.0 (10)	90
5	10.6	8.7 (90), 8.2 (20)	110
6	10.5	8.2 (130)	130
7	10.5	8.2 (150)	150
8	10.4	8.2 (170)	170
9	10.4	8.2 (190)	190
10	10.4	8.2 (210)	210
11	10.3	8.2 (230)	230

2 Bulk gelling experiments

These are all the gelling and non-gelling points that are represented in the scatter and ternary plots for the bulk gelling experiments of this thesis. They are separated according to the pH in the vials.

Here follows an explanation for what the description of the different columns mean:

Silica = The mass of the silica component added [g] (includes water)

wt% SiO_2 = The wt% of the silica added

wt% SiO_2 sample = The actual wt% silica in a non-gelling sample

wt% SiO_2 sample (gel) = The actual wt% silica in a gelling sample

It is the same for CNC but with CNC instead of silica.

These samples were photographed as they were investigated using the inverted test tube technique. All samples were examined using this technique. However, only those series of samples that contained samples that gelled were documented both inverted and non-inverted. The full set of samples follows below:

pH 10, 1 wt% CNC, 30 wt% silica

Sample	1	2	3	4	5	6	7	8	9	10	11
CNC [wt%]	1.00	0.90	0.80	0.70	0.60	0.50	0.40	0.30	0.20	0.10	0.00
Silica [wt%]	0.00	3.00	6.00	9.00	12.0	15.0	18.0	21.0	24.0	27.0	30.0

pH 8, 1 wt% CNC, 30 wt% silica (same wt% in the samples as in table for pH 10)

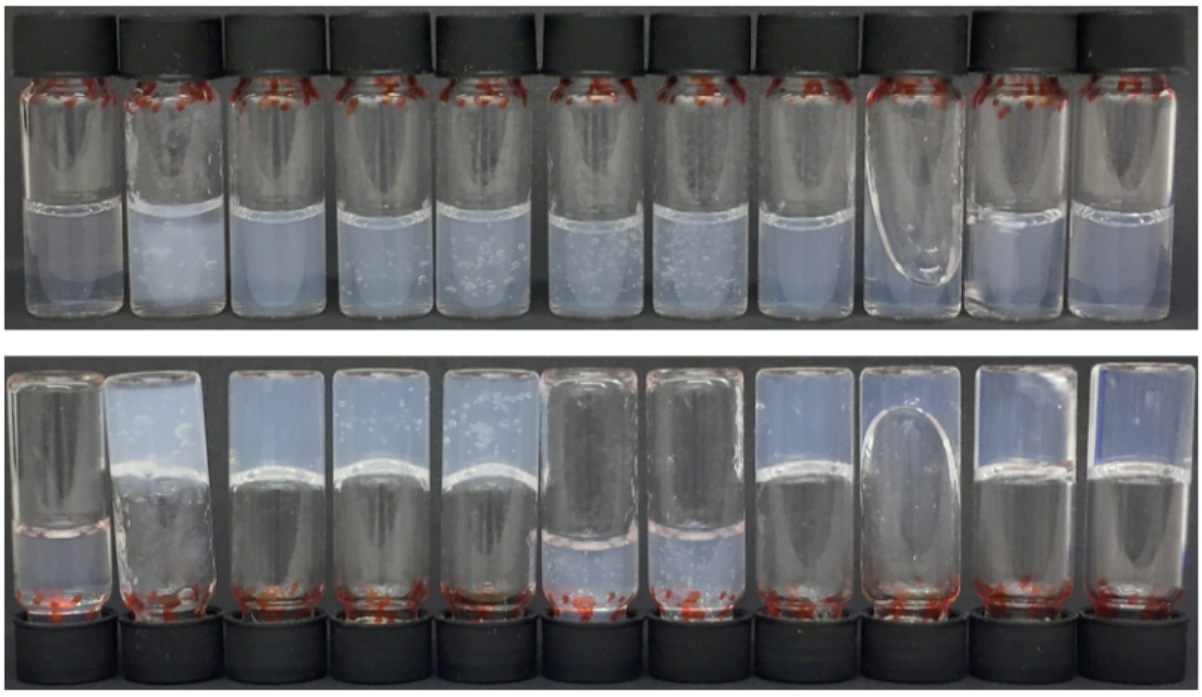

Sample	1	2	3	4	5	6	7	8	9	10	11

pH 6, 1 wt% CNC, 30 wt% silica (same wt% in the samples as in table for pH 10)

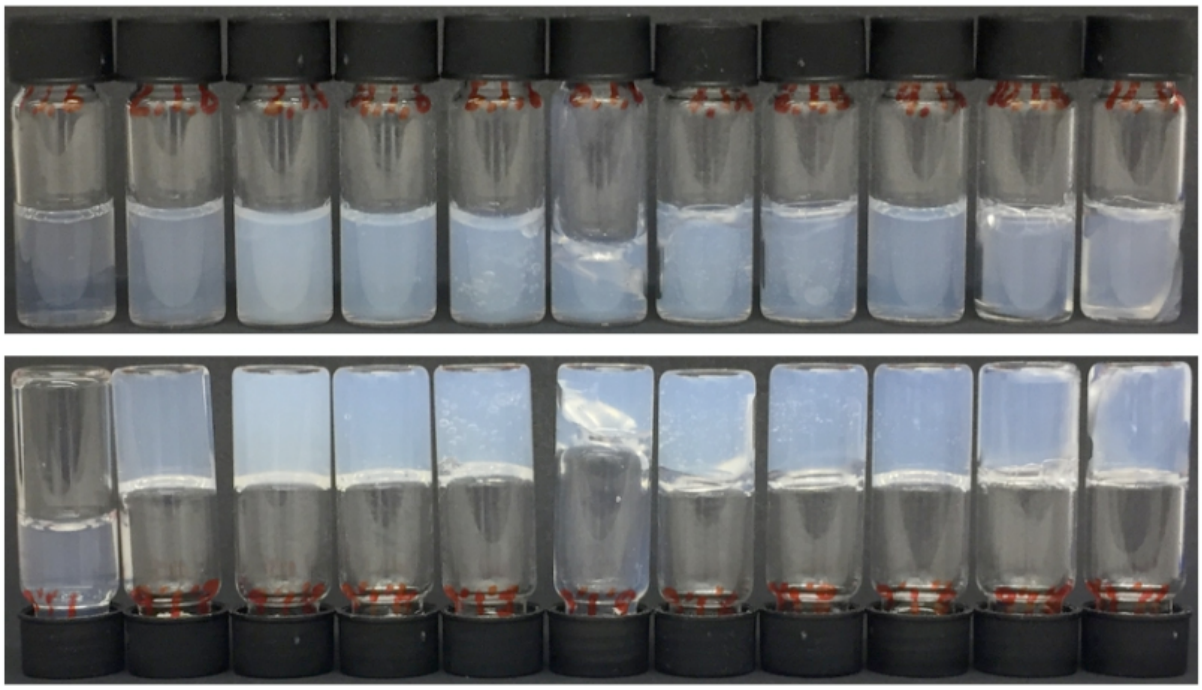

Sample	1	2	3	4	5	6	7	8	9	10	11

pH 4, 1 wt% CNC, 30 wt% silica (same wt% in the samples as in table for pH 10)

Sample	1	2	3	4	5	6	7	8	9	10	11

pH 10, 0.5 wt% CNC, 1 wt% Silica

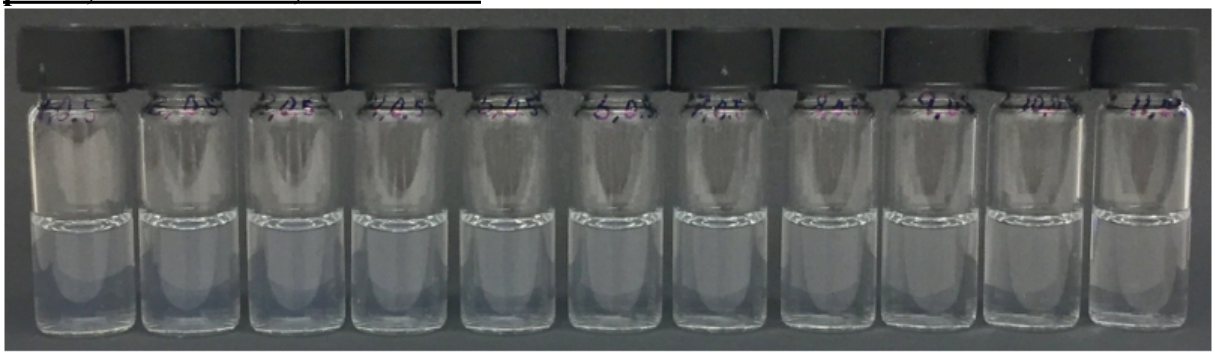

Sample	1	2	3	4	5	6	7	8	9	10	11
CNC [wt%]	0.50	0.45	0.40	0.35	0.30	0.25	0.20	0.15	0.10	0.05	0.00
Silica [wt%]	0.00	0.10	0.20	0.30	0.40	0.50	0.60	0.70	0.80	0.90	1.00

pH 8, 0.5 wt% CNC, 1 wt% silica (same wt% in the samples as in table for pH 10)

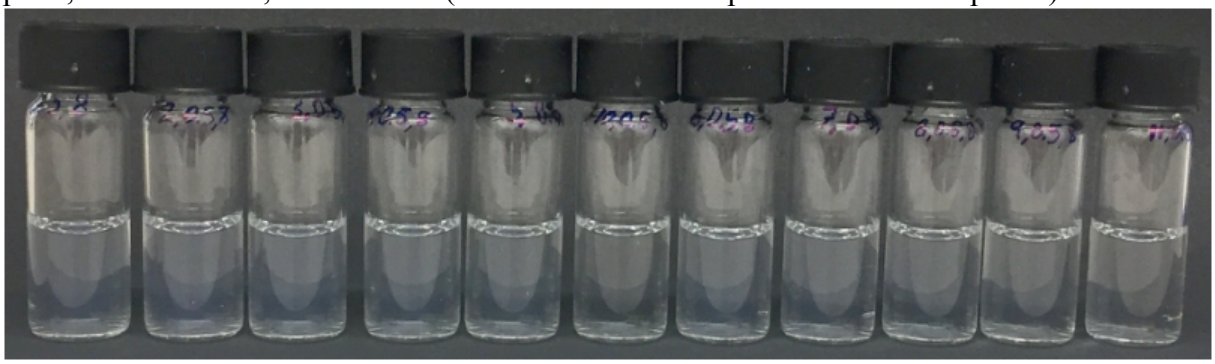

Sample	1	2	3	4	5	6	7	8	9	10	11

pH 6, 0.5 wt% CNC, 1 wt% silica (same wt% in the samples as in table for pH 10)

Sample	1	2	3	4	5	6	7	8	9	10	11

pH 4, 0.5 wt% CNC, 1 wt% silica (same wt% in the samples as in table for pH 10)

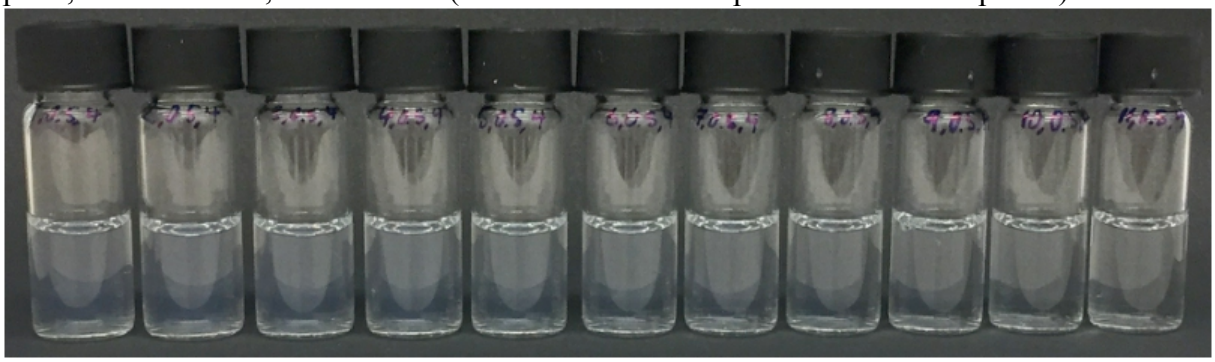

Sample	1	2	3	4	5	6	7	8	9	10	11

pH 10, 2 wt% CNC, 2 wt% silica (no gelling)

Sample	1	2	3	4	5	6	7	8	9	10	11
CNC [wt%]	2.00	1.80	1.60	1.40	1.20	1.00	0.80	0.60	0.40	0.20	0.00
Silica [wt%]	0.00	0.20	0.40	0.60	0.80	1.00	1.20	1.40	1.60	1.80	2.00

pH 8, 2 wt% CNC, 2 wt% silica (same wt% in the samples as in table for pH 10)

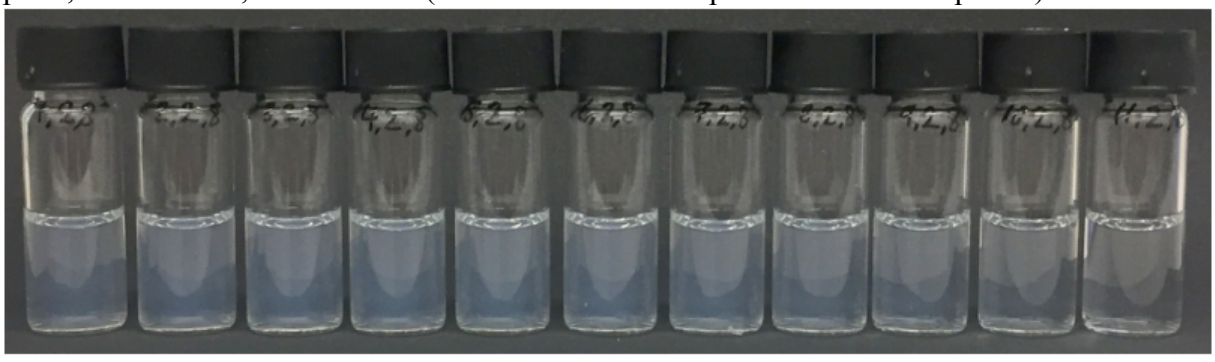

Sample	1	2	3	4	5	6	7	8	9	10	11

pH 6, 2 wt% CNC, 2 wt% silica (same wt% in the samples as in table for pH 10)

Sample	1	2	3	4	5	6	7	8	9	10	11

pH 4, 2 wt% CNC, 2 wt% silica (same wt% in the samples as in table for pH 10)

Sample	1	2	3	4	5	6	7	8	9	10	11

pH 10, 2 wt% CNC, 5 wt% silica (no gelling)

Sample	1	2	3	4	5	6	7	8	9	10	11
CNC [wt%]	2.00	1.80	1.60	1.40	1.20	1.00	0.80	0.60	0.40	0.20	0.00
Silica [wt%]	0.00	0.50	1.00	1.50	2.00	2.50	3.00	3.50	4.00	4.50	5.00

pH 8, 2 wt% CNC, 5 wt% silica (same wt% in the samples as in table for pH 10)

Sample	1	2	3	4	5	6	7	8	9	10	11

pH 6, 2 wt% CNC, 5 wt% silica (same wt% in the samples as in table for pH 10)

Sample	1	2	3	4	5	6	7	8	9	10	11

pH 4, 2 wt% CNC, 5 wt% silica (same wt% in the samples as in table for pH 10)

Sample	1	2	3	4	5	6	7	8	9	10	11

pH 10, 2 wt% CNC, 10 wt% silica

Sample	1	2	3	4	5	6	7	8	9	10	11
CNC [wt%]	2.00	1.80	1.60	1.40	1.20	1.00	0.80	0.60	0.40	0.20	0.00
Silica [wt%]	0.0	1.0	2.0	3.0	4.0	5.0	6.0	7.0	8.0	9.00	10.0

pH 8, 2 wt% CNC, 10 wt% silica (same wt% in the samples as in table for pH 10)

Sample	1	2	3	4	5	6	7	8	9	10	11

pH 6, 2 wt% CNC, 10 wt% silica (same wt% in the samples as in table for pH 10)

Sample	1	2	3	4	5	6	7	8	9	10	11

pH 4, 2 wt% CNC, 10 wt% silica (same wt% in the samples as in table for pH 10)

Sample	1	2	3	4	5	6	7	8	9	10	11

pH 10, 2 wt% CNC, 15 wt% silica

Sample	1	2	3	4	5
CNC [wt%]	1.60	1.00	0.40	0.20	0.00
Silica [wt%]	3.00	7.50	12.0	13.5	15.0

pH 8, 2 wt% CNC, 15 wt% silica (same wt% in the samples as in table for pH 10)

Sample	1	2	3	4	5

pH 6, 2 wt% CNC, 15 wt% silica (same wt% in the samples as in table for pH 10)

Sample	1	2	3	4	5

pH 4, 2 wt% CNC, 15 wt% silica (same wt% in the samples as in table for pH 10)

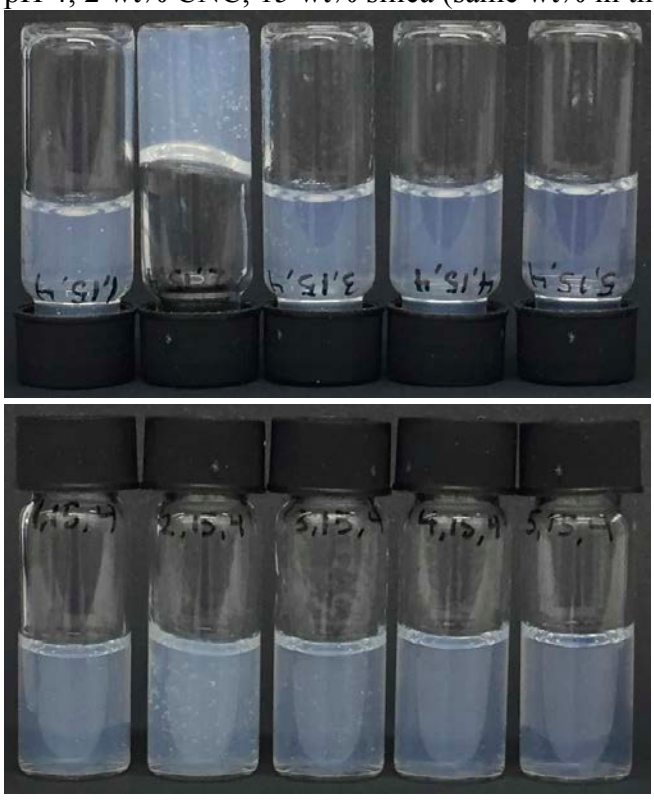

Sample	1	2	3	4	5

pH 10, 2 wt% CNC, 20 wt% silica

Sample	1	2	3	4	5	6
CNC [wt%]	1.40	1.20	1.00	0.80	0.20	0.00
Silica [wt%]	6.00	8.00	10.0	12.0	18.0	20.0

pH 8, 2 wt% CNC, 20 wt% silica (same wt% in the samples as in table for pH 10)

Sample	1	2	3	4	5	6

pH 6, 2 wt% CNC, 20 wt% silica (same wt% in the samples as in table for pH 10)

Sample	1	2	3	4	5	6

pH 4, 2 wt% CNC, 20 wt% silica (same wt% in the samples as in table for pH 10)

pH 10, 2 wt% CNC, 25 wt% silica

Sample	1	2	3	4
CNC [wt%]	1.00	0.80	0.60	0.00
Silica [wt%]	12.5	15.0	17.5	25.0

pH 8, 2 wt% CNC, 25 wt% silica (same wt% in the samples as in table for pH 10)

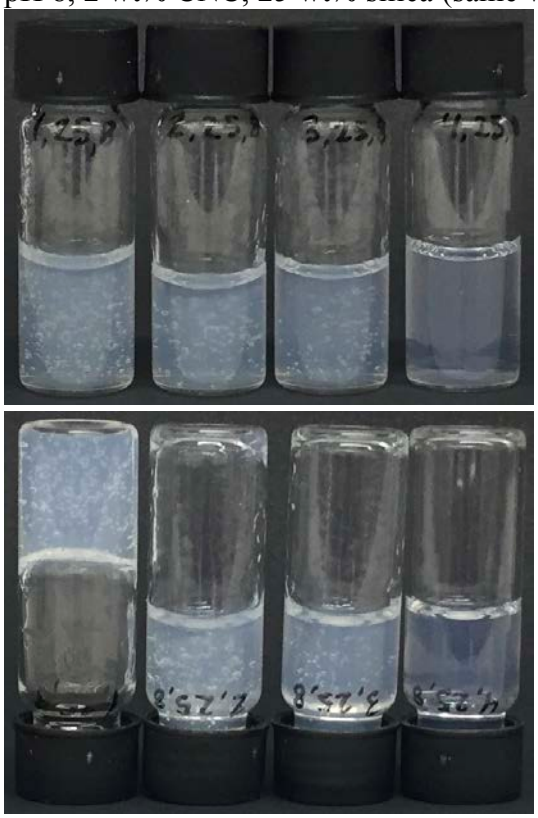

Sample	1	2	3	4

pH 6, 2 wt% CNC, 25 wt% silica (same wt% in the samples as in table for pH 10)

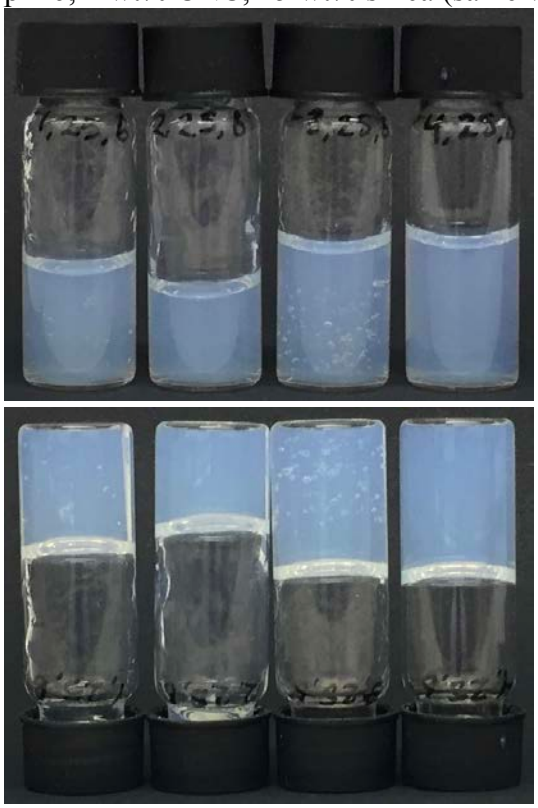

Sample	1	2	3	4

pH 4, 2 wt% CNC, 25 wt% silica (same wt% in the samples as in table for pH 10)

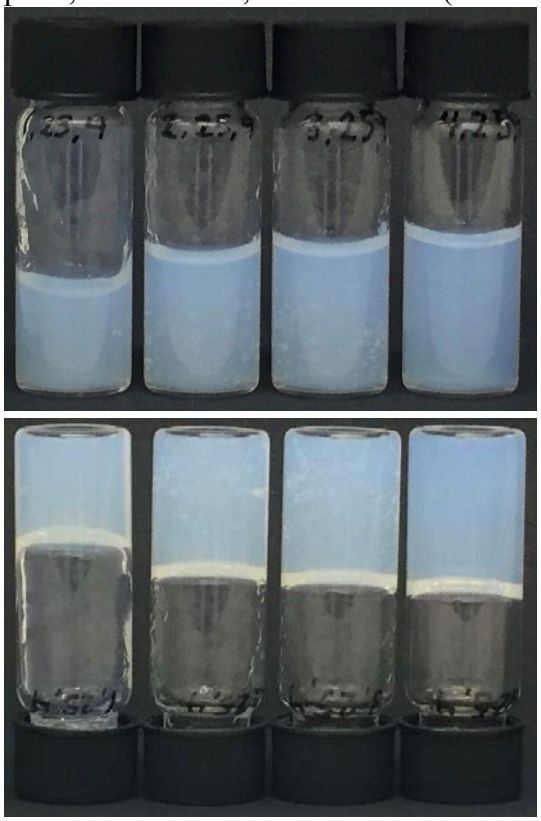

Sample	1	2	3	4

<u>pH 10, 2 wt% CNC, 30 wt% silica</u>

Sample	1	2	3	4	5
CNC [wt%]	1.60	1.40	1.20	1.00	0.80
Silica [wt%]	6.00	9.00	12.0	15.0	18.0

pH 8, 2 wt% CNC, 30 wt% silica (same wt% in the samples as in table for pH 10)

Sample	1	2	3	4	5

pH 6, 2 wt% CNC, 30 wt% silica (same wt% in the samples as in table for pH 10)

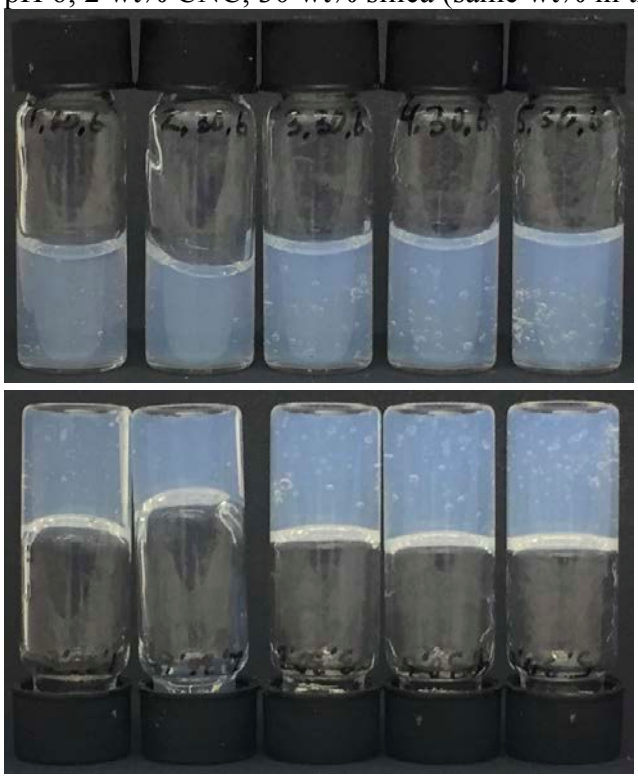

Sample	1	2	3	4	5

pH 4, 2 wt% CNC, 30 wt% silica (same wt% in the samples as in table for pH 10)

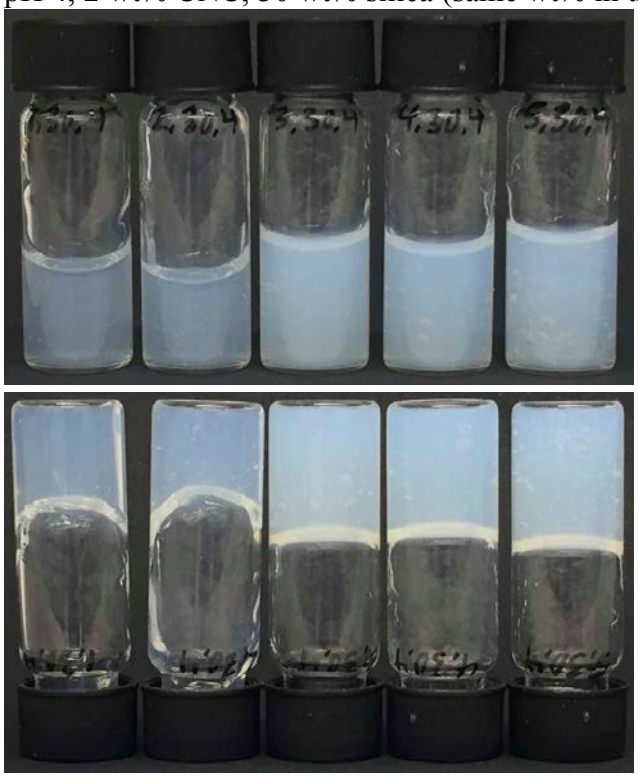

Sample	1	2	3	4	5

Table A.3: Masses of $CaCl_2$ addition at pH 6, 4 and 2.

pH sample	flask [wt% $CaCl_2$]	m [g] ($CaCl_2$)	m [g] (total)
pH 6	10	2.01	20.03
pH 4	10	2.00	20.28
pH 2	10	2.01	20.04

Upon extruding sample 2 with 6 wt% silica and 1.6 wt% CNC to the vial with pH 6 instant gelling could be observed. The gelling behaviour was indistinguishable at pH 4 and 2. In all the different vials (different pHs) the fibres formed were impossible to retrieve from the liquid with the needle as they broke when being dragged to the surface, through it and up on the sides of the vials.

3 Studies of gelling behaviour with $CaCl_2$ at pH 4

To study the effect that $CaCl_2$ could have on gelling at pH 6 four different samples were prepared.

Table A.4: Masses of $CaCl_2$ addition at pH 4.

Sample	flask [wt% $CaCl_2$]	m [g] granular $CaCl_2$ (calculated)	m [g] ($CaCl_2$) (weighed)	m [g] (total)
1	7.5	0.075*20 = 1.5	1.48	19.99
2	5.0	0.050*20 = 1.0	1.00	19.97
3	2.5	0.025*20 = 0.5	0.50	20.02
4	1.0	0.010*20 = 0.2	0.20	20.05

2 ml from the samples above were added to 4 different 4 ml vials (one for each sample) to prepare the four different baths for the gelling. The observations for samples 1 to 4 were as follows:

1. 7.5 wt% $CaCl_2$.Instant gelling. Better than 10 wt% studied earlier. Breaks upon collection however.
2. 5.0 wt% $CaCl_2$. The gelling is instant and very similar to that at 7.5 wt%. The gel behaves slightly better (less brittle)
3. 2.5 wt% $CaCl_2$. Best one yet. Almost collectible.
4. 1.0 wt% $CaCl_2$. About the same as for 2.5 wt%.

4 The effect of different $CaCl_2$ concentrations on gelling

To study the behaviour of silica and CNC further three different samples were prepared using 2 wt% CNC and 2 wt% silica. These were:

1. 2 wt% CNC
2. 2 wt% CNC and 2 wt% silica in a 50/50 wt% mixture
3. 2 wt% silica

Then 15 different vials were prepared to study the gelling. These vials contained 10 wt%, 5.0 wt%, 2.5 wt% or 1.0 wt% $CaCl_2$. There were 3 of each $CaCl_2$ concentration.

45 ml stock solutions were prepared for each of the salt concentrations. The different concentrations for $CaCl_2$ were prepared by mixing granular $CaCl_2$ in a HCl mixture with pH They were prepared as follows:

1. 10 wt% = 0.10*45 = 4.5 g (of $CaCl_2$)

2. 7.5 wt% = 0.075*45 = 3.375 g (of $CaCl_2$)

3. 5.0 wt% = 0.050*45 = 2.25 g (of $CaCl_2$)

4. 2.5 wt% = 0.025*45 = 1.125 g (of $CaCl_2$)

5. 1.0 wt% = 0.010*45 = 0.45 g (of $CaCl_2$)

1. 2 wt% CNC Approximately 3 ml from Sample 1 with 2 wt% CNC was added to 5 different vials each with 15 ml of one of the five $CaCl_2$ concentrations above. The 2 wt% CNC behaved very similarly in all the vials (no gelling).

2. 2 wt% CNC and 2 wt% silica in a 50/50 wt% mixture.

10 wt% SiO2 vial: a somewhat continuous fibre that loses its structure within approximately 5 seconds

7.5 wt%, 5.0 wt%, almost the same as for 10 wt% but with a bit less stable gel.

2.5 wt%, almost fully dissolving. No gelling.

1.0 wt%, fully dissolving and no gelling.

3. 2 wt% silica. At all the different $CaCl_2$ concentrations the silica is completely dissolved in the vials. No gelling at all.

5 The impact of $CaCl_2$ addition at pH 6

To study the effect that granular $CaCl_2$ could have on gelling at pH 6 four different samples were prepared. These were:

1. 7.5 wt% = 0.075*20 = 1.5 g (of $CaCl_2$)

2. 5.0 wt% = 0.050*20 = 1.0 g (of $CaCl_2$)

3. 2.5 wt% = 0.025*20 = 0.5 g (of $CaCl_2$)

4. 1.0 wt% = 0.010*20 = 0.2 g (of $CaCl_2$)

Table A.5: Masses of $CaCl_2$ addition at pH 6.

Sample	flask [wt% CaCl2]	m [g] (CaCl2)	m [g] (total)
1	7.5	1.51	19.99
2	5.0	0.99	20.09
3	2.5	0.52	19.96
4	1.0	0.21	20.01

A new sample 2 (6 wt% SiO_2, 1.6 wt% CNC) was prepared by mixing 0.4 g 30 wt% SiO_2 solution with a 1.6 wt% CNC solution to get a sample of 2 g (approximately 2 ml).

2 ml from the samples above were added to 4 different 4 ml vials (one for each sample) to prepare the four different baths for the gelling. The observations for samples 1 to 4 were as follows:

1. 7.5 wt% $CaCl_2$.Instant gelling and the gel floats initially. The fibres that formed were almost collectible but not quite.

2. 5.0 wt% $CaCl_2$. The gelling is instant but this time the gel sinks instantly. The fibres that formed are in small pieces (up to 2 mm) and are somewhat collectible

3. 2.5 wt% $CaCl_2$. The same behaviour as for sample 2 (5.0 wt% $CaCl_2$).

4. 1.0 wt% $CaCl_2$. The gelling is instant and the gel sinks to the bottom of the vial. The fibres are not very collectible.

6 Gelling at pH 4 with a 5 wt% $CaCl_2$/HCl mixture at pH 4

85 ml of the 5 wt% $CaCl_2$/HCl mixture at pH 4 was prepared.

5 wt% = 0.050*85 g = 4.25 g

m(CaCl2) = 4.25 g weighed = 4.25 g

m(total) = 85 g weighed = 85.00 g

The sample was stirred for 30 minutes to completely dissolve the $CaCl_2$.

CNC/Silica mixtures

Table A.6: Different silica/CNC mixtures at pH 4.

Sample	m [g], wt% SiO2 component	m [g], wt% CNC component	wt% SiO2, sample	wt% CNC, sample
1	0.4 g, 30 wt%	1.6 g, 2 wt%	6 wt%	1.6 wt%
2	1.0 g, 20 wt%	1.0 g, 2 wt%	10 wt%	1.0 wt%
3	1.2 g, 30 wt%	0.8 g, 2 wt%	18 wt%	0.8 wt%
4	1.4 g, 30 wt%	0.6 g, 1 wt%	21 wt%	0.3 wt%
5	1.8 g, 30 wt%	0.2 g, 1 wt%	27 wt%	0.1 wt%

2 g (approximately 2 ml) of each of the samples in Table A.6 were prepared by mixing the two components in 5 different 4 ml vials.

15 ml from the 5 wt% $CaCl_2$ solution prepared earlier was added to 5 separate 30 ml vials in which the gelling were to be studied.

0.7 ml of each sample was extruded into the bath using a 0.80 x 80 mm needle. The observations follow below. The extrusion was done by hand at an approximate flow of 0.02 ml/s i.e. the syringe (0.6 ml) was emptied in approximately 30 seconds. Upon extruding the needle was circled in the bath and also moved from the bottom to the top in the vial. The observations for the samples were as follows:

1. Instant gelling but the fibres were not collectible. The longest fibres had a length of approximately 0.5 cm.

2. Instant gelling and the fibres are almost collectible. The longest fibres were decently stable and approximately 1 cm long. The fibres were extruded while moving the syringe from the bottom to the top of the vial. This was the most promising of the two samples.

7 Gelling in dish (10 wt% silica, 1 wt% CNC)

To study the gelling when sample 2 (10 wt% silica, 1 wt% CNC) was extruded and gelled in the bath another bath was prepared using a dish with a 7 cm diameter. This dish contained 50 ml 5 wt% $CaCl_2$ dissolved at pH 4. The 5 wt% $CaCl_2$ was prepared by mixing granular $CaCl_2$ (Aldrich) in a HCl mixture with pH 4.

5 wt%: 0.050*50 g = 2.50 g (of granular $CaCl_2$)

m(CaCl2) = 2.50 g weighed = 2.52 g

m(total) = 50 g weighed = 50.00 g

When extruded into the mixture the silica/CNC mixture gels instantly and over two seconds the fibre could be seen turning white. The fibres that are formed in the dish are quite solid but no attempt to be collect them were made at this stage.

8 Calcination of samples for SEM

To study the structure of the fibres using SEM they had to be collected and dried.

Sample 1 to 5 was prepared (2 g of each sample) in the following manner:

Table A.7.1: Preparation of silica/CNC samples for SEM

Sample	m [g], wt% SiO2 component	m [g], wt% CNC component	wt% SiO2, sample	wt% CNC, sample
1	0.4 g, 30 wt%	1.6 g, 2 wt%	6 wt%	1.6 wt%
2	1.0 g, 20 wt%	1.0 g, 2 wt%	10 wt%	1.0 wt%
3	1.2 g, 30 wt%	0.8 g, 2 wt%	18 wt%	0.8 wt%
4	1.4 g, 30 wt%	0.6 g, 1 wt%	21 wt%	0.3 wt%
5	1.8 g, 30 wt%	0.2 g, 1 wt%	27 wt%	0.1 wt%

Sample 6, which is similar to sample 2 but using CNF (0.35 wt%) instead of 1.0 wt% CNC, was prepared.

Table A.7.2: Preparation of silica/CNC samples for SEM

Sample	m [g], wt% SiO2 component	m [g], wt% CNF component	wt% SiO2, sample	wt% CNF, sample
6	1.0 g, 10 wt%	1.0 g, 0.35 wt%	5 wt%	0.175 wt%

For the gelling a 50 ml $CaCl_2$ solution was required for each sample. Therefore, 50 ml*6 = 300 ml 5 wt% $CaCl_2$/HCl solution was prepared:

5 wt%= 0.050*300 g =15.0 g

m(CaCl2) = 15.0 g, weighed 15.02 g

m(total) = 300 g, weighed = 300.04 g

The mixture was set to stir for 60 minutes.

0.7 ml of each sample was gelled (one at a time) in a dish containing 50 ml $CaCl_2$ solution at pH 4. The dish was emptied after the required amount of the gelled mixture had been retrieved from the gelling bath.

1.The sample was gelled in the dish and left for 2 minutes before it was collected. The pieces that were collected were small (around 1 cm long).

2. In this sample the fibres were a bit longer (around 2 cm) but more brittle and thereby more difficult to collect.

3.Very similar to sample number 2.

4. Extremely poor at forming fibres. More like a mist. A few fibre pieces could be collected.

5. Much longer fibres than for sample 4. Somewhat collectible.

6. Similar physical properties as observed for fibre 5 but whiter in colour.

As stated, a few strands or pieces the fibres were collected and placed in ceramic beakers for the calcination and on teflon plates for drying in room temperature.

The samples in the ceramic beakers for the calcination were placed in an oven (Nabertherm P 330) and were set to heat in the manner below:

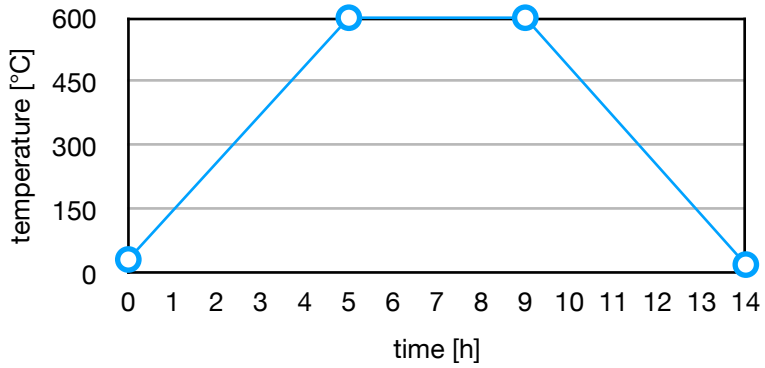

Figure A.1: Heating graph for calcination at 600°C.

The oven was started and set to run for 4 hours at 600°C to get rid of all water and the CNC still in the sample. The ramp up of the temperature to 600°C was set to 5 hours. The oven was automatically turned off after 9 hours and left to cool itself to room temperature (21°C).

The samples were then retrieved from the oven. They had dried and mostly kept their shape. The beakers were then covered with aluminium foil to protect the samples.

All the samples were collected and placed in 12 different 4 ml vials (6 for calcined samples and 6 for samples dried at room temperature. Most of the fibres retained their shape after being transferred to the vials but some were quite brittle and broke into smaller pieces.

9 Spinnability of CNF

To examine the spinnability of CNF new samples were prepared. These were:

Table A.8: Preparation of CNF mixtures (100-90 wt%).

Sample (dw before calcination)	m(CNF) [g]	m(SiO_2) [g]	m(total)
100 wt% CNF	10.02	---	10.02
97 wt% CNF	10.00	10.20	20.20
95 wt% CNF	10.02	17.35	27.37
90 wt% CNF	10.01	36.70	46.71

Upon mixing the samples they had bubbles in them that had to be removed by centrifuging the samples. First the mixtures were transferred to 15 ml centrifuge tubes using a 5000 µl pipette. The tubes were then put into the centrifuge (Heraeus Sepatech) at 1600 rpm for 60 seconds. After the centrifuging the bubbles were gone.

15 ml $CaCl_2$ (pH 2) mixture was added to each of four different vials and the first sample was gelled in the first vial using a syringe. The same procedure was repeated for the remaining experiments.

These were the observations for the different samples:

100% CNF: The fibre formed was very stable and could easily be collected on the side of the vial. However, the fibre did not stick to the side of the vial and slid down into the bath again. One long fibre.

97% CNF: Very similar to 100% CNF. Formed long fibres but more than one. The fibres broke apart somewhat upon collection but this could be attributed to the collection method using the needle.

95% CNF: Similar to 97% CNF. Formed more than one long fibre. Some small lumps formed as well. The fibres could easily be retrieved from the gelling bath but fell down from the sides into the gelling bath again.

90% CNF: Formed fibres but these were more brittle than before. These broke somewhat upon collection. Several lumps also formed that could not be collected and broke apart upon attempts to collect them. The lumps were not meant to be collected and this was just done to examine the properties.

10 SEM analysis

The samples were coated with palladium using the Emitech K550X. The coater was run for 3 minutes at 25 mA. The samples were then analysed using the JSM-7800F SEM. The surface offset was set to 5 mm.

11 Additional SEM images

11.1 80 wt% SiO_2, 20 wt% CNC

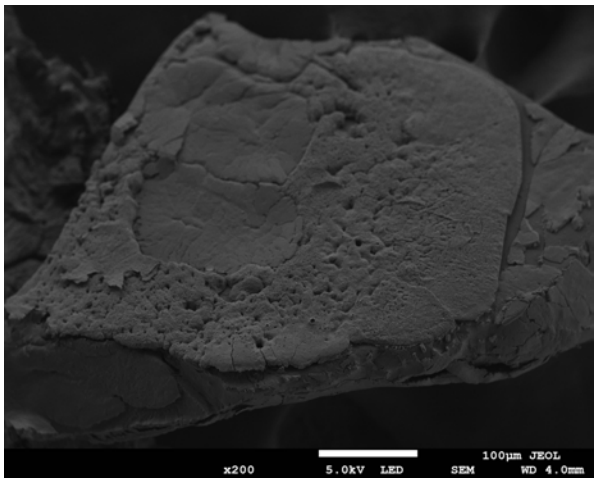

80 wt% SiO_2, 20 wt% CNC (non-calcined)

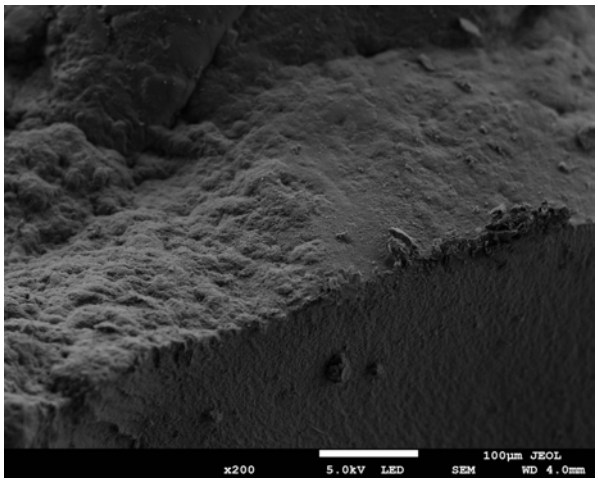

80 wt% SiO_2, 20 wt% CNC (calcined)

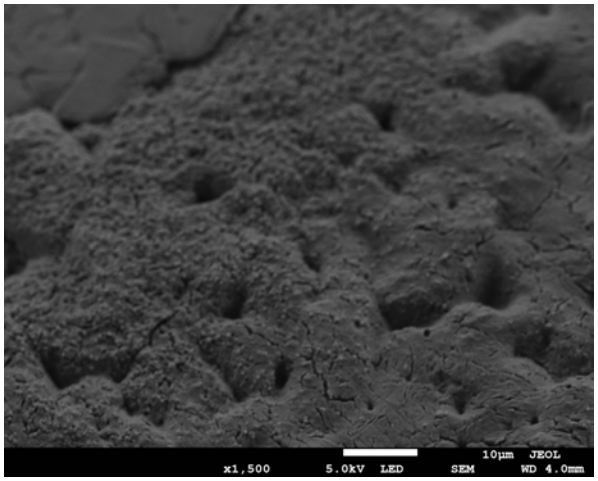

80 wt% SiO_2, 20 wt% CNC (non-calcined)

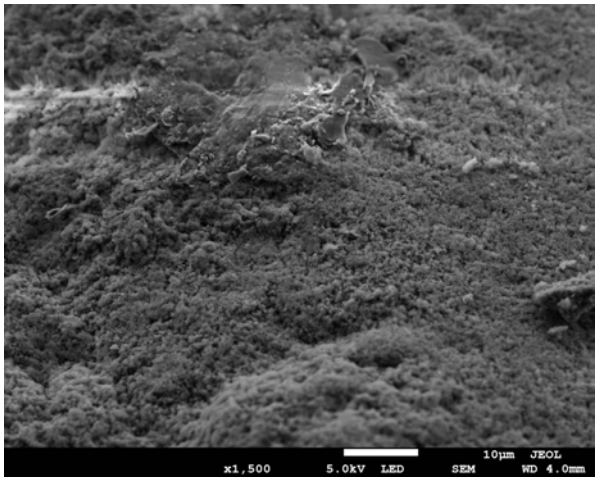

80 wt% SiO_2, 20 wt% CNC (calcined)

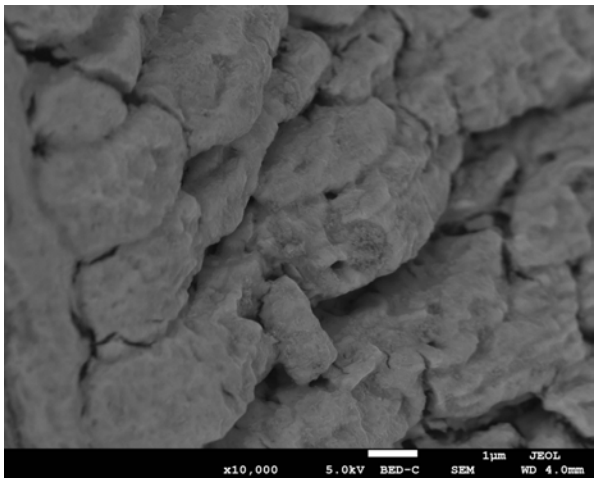

80 wt% SiO_2, 20 wt% CNC (non-calcined)

11.2 50 wt% SiO_2, 50 wt% CNC

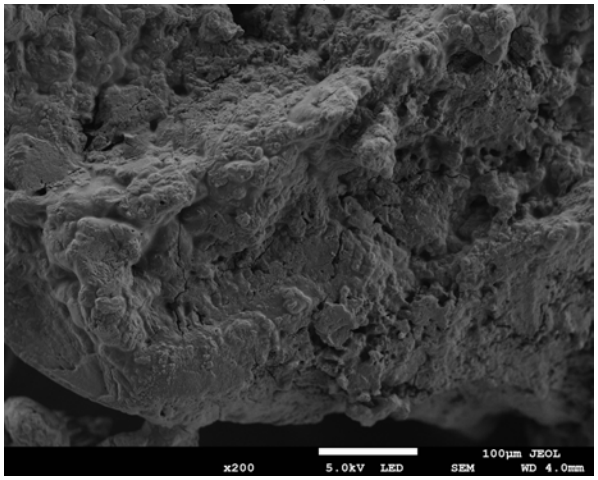

50 wt% SiO_2, 50 wt% CNC (non-calcined)

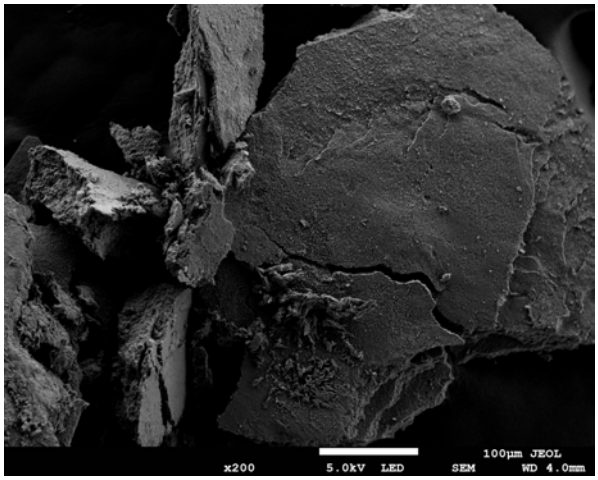

50 wt% SiO_2, 50 wt% CNC (calcined)

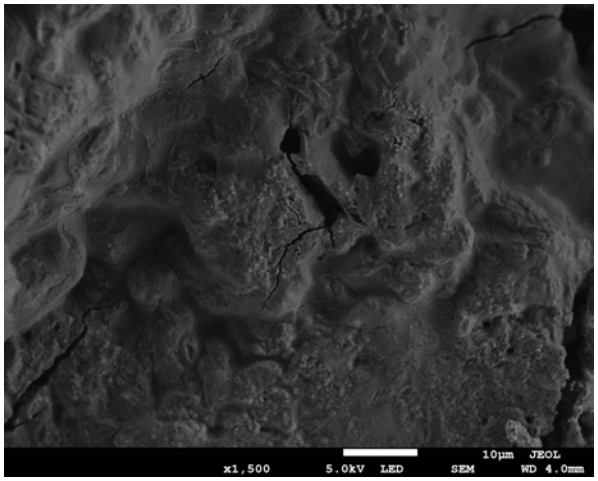

50 wt% SiO_2, 50 wt% CNC (non-calcined)

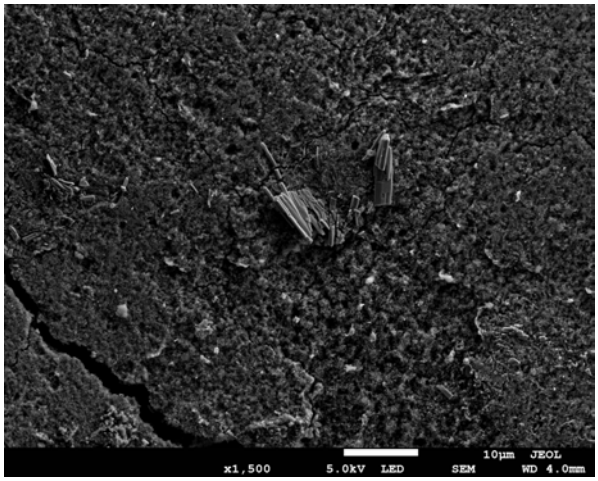

50 wt% SiO_2, 50 wt% CNC (calcined)

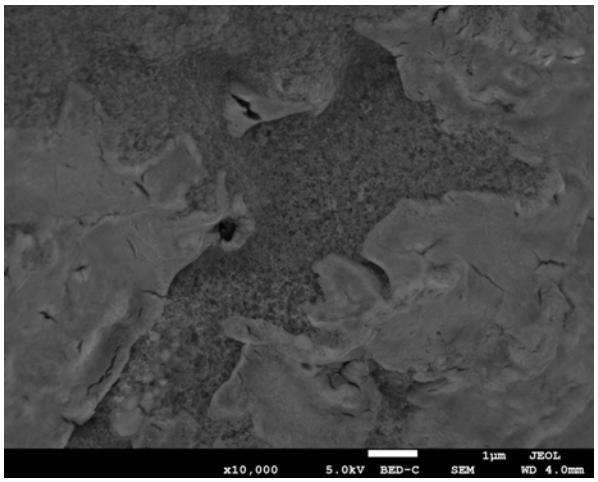

50 wt% SiO_2, 50 wt% CNC (non-calcined)

11.3 20 wt% SiO_2, 80 wt% CNC

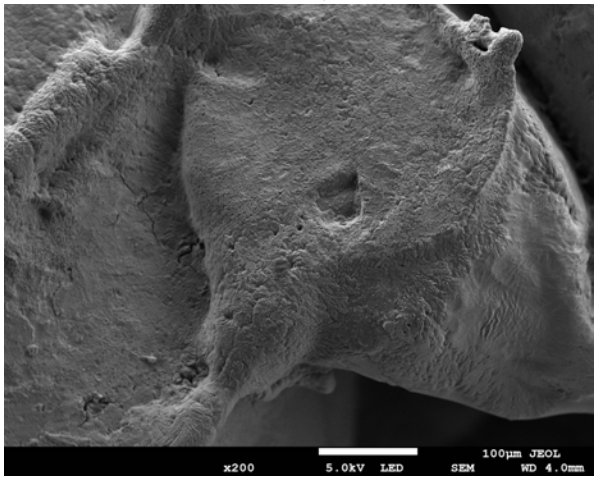

20 wt% SiO_2, 80 wt% CNC (non-calcined)

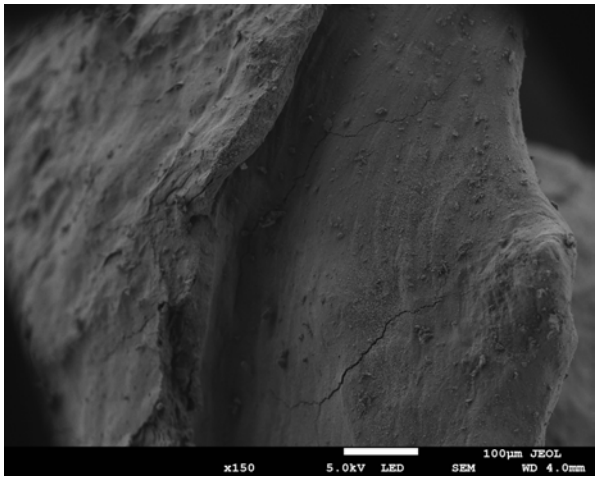

20 wt% SiO_2, 80 wt% CNC (calcined)

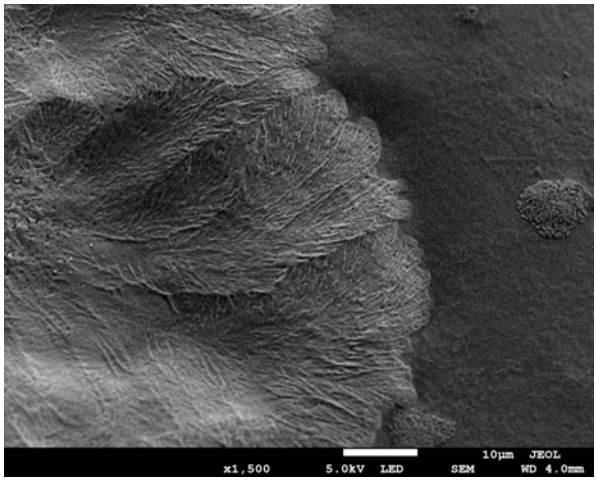

20 wt% SiO_2, 80 wt% CNC (non-calcined)

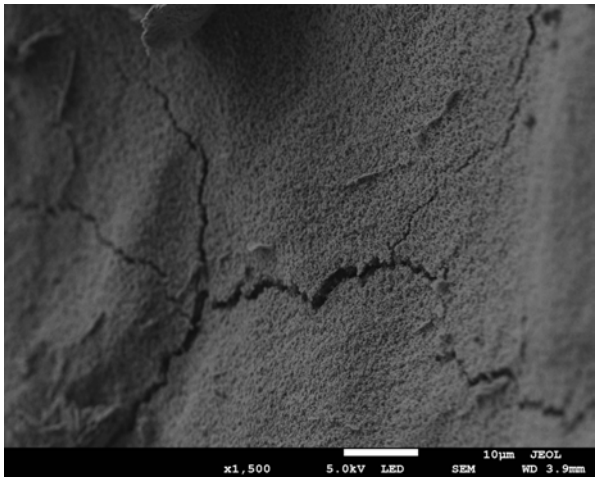

20 wt% SiO_2, 80 wt% CNC (non-calcined)

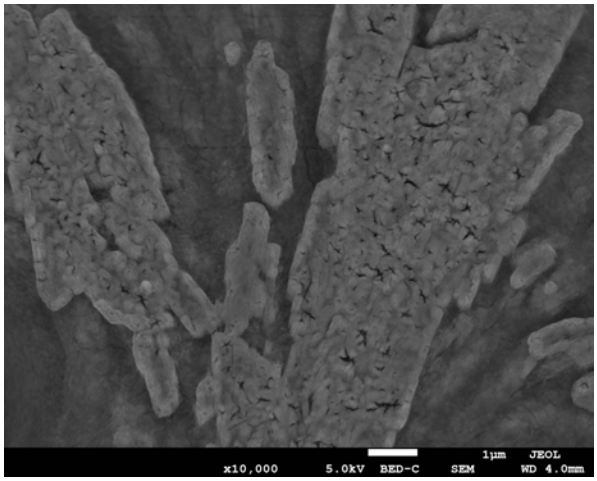

20 wt% SiO_2, 80 wt% CNC (non-calcined)

12 Spinnability of CNF

To further study the spinnability of CNF four other mixtures of CNF and silica were considered. These were:

Table A. 9: Preparation of CNC samples for spinnability testing (80-40 wt%)

Sample	0.35 wt% CNF [g]	30 wt% SiO_2 [µl]
80 wt% CNF	10.00	24.31
60 wt% CNF	10.00	41.67
50 wt% CNF	10.00	64.83
40 wt% CNF	10.00	97.21

80% CNF: Mostly lumps are formed but also some fibres that are quite collectible and stable.

70% CNF: Not many lumps. Two long fibres are formed. These two fibres are collectible but but also quite brittle and breaks relatively easily upon collection.

60% CNF: Similar to 70% but forms more lumps and fibres that are more brittle.

50% CNF: Not many lumps formed. The fibres that form are even more brittle and breaks somewhat upon collection.

13 Sample preparation for nitrogen sorption analysis

Two new samples were prepared.

Table A.10: Sample preparation for nitrogen sorption analysis.

Sample	m [g], wt% SiO_2 component	m [g], wt% CNC component	wt% SiO_2, sample	wt% CNC, sample
1	4.0 g, 30 wt%	16 g, 2 wt%	6 wt%	1.6 wt%
2	18 g, 30 wt%	2.0 g, 2 wt%	27 wt%	0.1 wt%

For the gelling a new $CaCl_2$/HCl solution had to be prepared.

5 wt% = 0.05*200=10 g

m($CaCl_2$) = 10 g, weighed 10.00 g

m(total) = 200 g, weighed = 200.06 g

The mixture was set to stir for 10 minutes until all the $CaCl_2$ had been dissolved. The CNC samples (sample 1 and 2) were gelled in a pH 4 bath with $CaCl_2$ and the CNF samples (sample 3,4 and 5) were gelled in a bath with pH 2. The CNF samples had been mixed earlier.

Table A.11: CNF samples for nitrogen sorption analysis.

Sample	wt% SiO_2, sample	wt% CNF, sample
3	3 wt%	97 wt%
4	10 wt%	90 wt%
5	30 wt%	70 wt%

The samples were gelled in their respective baths and collected.

The samples were then calcined and collected.

Sample 1 and 2 had dried and could be collected. Sample 3, 4 and 5, however, had almost no mass left after calcination.

Sample 1 and 2 were collected:

Sample 1 weight 0.054 g = 54 mg SiO2

Sample 2 weight 0.143 g = 143 mg SiO2

Approximately 300 mg of each sample is needed for the sorption analysis so this was not enough.

14 Collection using vacuum suction

The new approach was to use a beaker with a filter (Whatman TM 70 mm) filtering the $CaCl_2$/ fibre mixture under suction and then collecting the fibres from the paper.

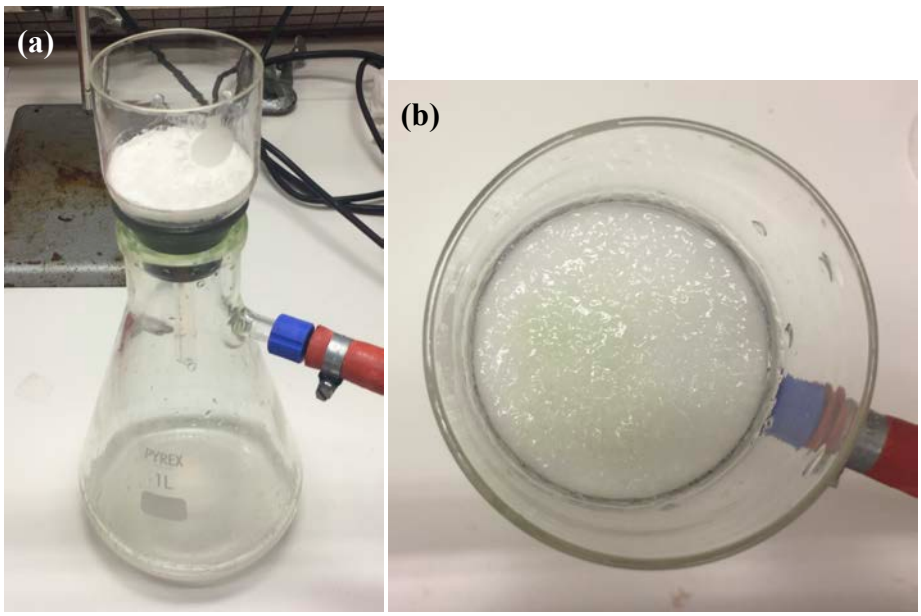

Figure A.2: **(a)** Vacuum suction setup and **(b)** a magnified view of part of the setup.

For the gelling a new $CaCl_2$/HCl solution had to be prepared.

5 wt% = 0.05*500 = 20 g

m(CaCl2) = 25 g, weighed 25.04 g

m(total) = 500 g, weighed = 499.99 g

The mixture was set to stir for 1 hour to fully dissolve and mix the $CaCl_2$.

The samples were gelled in the $CaCl_2$ bath using the syringe pump set to a flow of 3 ml/min i.e. 0.05 ml/s. The mixture was gelled in a dish as before but the collection was done by pouring the mixture over a filter attached to a suction setup. The "fibres"/gel was then put into vials and put to dry in room temperature overnight.

Preparation of 2 wt% CNC. 500 g was needed.

2 wt% = 0.02*500 g = 10 g

m(CNC) = 10 g, weighed = 9.98 g

m(total) = 500 g, weighed = 500.28 g

The mixture was set to stir for four hours. The mixture was then set to be sonicated for 5 min three times at 30% amplitude.

Table A.12: Preparation of SiO_2 /CNC mixtures 79 wt%, 88.24 wt% and 99.63 wt%.

Sample	m [g], wt% SiO_2 component	m [g], wt% CNC component	dry wt% SiO_2, sample	dry wt% CNC, sample
1	4.0 g, 30 wt%	16 g, 2 wt%	79	21
2	20 g, 2 wt%	20 g, 2 wt%	50	50
3	8 g, 2 wt%	32 g, 2 wt%	20	80
4	2 g, 30 wt%	18 g, 1 wt%	88.24	11.76
5	18 g, 30 wt%	2 g, 1wt%	99.63	0.3690

200 ml 2 wt% SiO_2 solution was prepared from the 30 wt% stock solution.

13.33 ml 30 wt% SiO_2 was mixed with 186.67 ml distilled water.

The mixture was left to stir for 5 minutes.

All the mixtures were prepared by mixing according to the ratios specified in Table A.12.

The samples were then gelled in a dish with 5 wt% $CaCl_2$ and collected by being poured onto a filter and separated used vacuum suction. Sample 1, 4 and 5 held together quite well and could be collected using a 4 mm wide spatula.

After the samples had been collected i the beakers they were put in the oven for calcination at 600°C.

All the samples from the calcination were then collected.

15 Nitrogen sorption analysis

Sample 1, 2 and 3 were selected and weighed. First the empty tube was weighed and then the tube with the sample in was weighed.

The sample was put for drying in the Micrometrics Smartprep for 90°C for 1 hour and then 200°C for 3 hours. The tubes were put in the dryer with one N_2 pipe in each and and the lids put into the tubes. After the drying the tubes were removed and the lids pushed closed. Lastly the sample was weighed after being dried in N_2. The weight before and after the drying is represented in Table A.13.

Table A.13: Drying of samples for nitrogen sorption analysis

Sample	weight before drying [g]	weight after drying [g]	weight difference [%]
1	0.2894	0.2859	0.06084
2	0.2359	0.2228	2.856
3	0.2315	0.2167	3.302

After the drying the samples were put into the nitrogen sorption analysis (Tristar 3000). This was done by first pouring liquid nitrogen into a large beaker and then screwing the three samples to the machine. The nitrogen beaker was then placed below the samples in position to later be automatically rised to cool the samples during the measurements. The calculated mass of the samples (after drying) was put into the system and the nitrogen sorption was left to run for 12 hours.

Preparation of additional CNF samples for nitrogen sorption analysis.

Table A.14: Additional CNF samples for nitrogen sorption analysis (79 wt% SiO_2, 21 wt% CNF)

Sample	m [g], wt% SiO_2 component	m [g], wt% CNF component	wt% SiO_2, sample	wt% CNF, sample	dry wt% SiO_2, sample	dry wt% CNF, sample
1	26.33 g, 2 wt%	40 g, 0.35 wt%	6 wt%	1.6 wt%	79	21

The sample was shaken to mix its contents and then set to stir for 10 minutes to mix it further. The mixture had some bubbles in it so it had to be centrifuged. The mixture was transferred to six 15 ml centrifuge tubes and then centrifuged at 1600 rpm for 1 minute.

The mixture was then gelled in a dish (7 cm diameter) and then collected using a filter under vacuum suction and finally collected using a 4 mm wide spatula.

The fibres/gel formed were very transparent but held together well and could be easily collected as they it did not break apart.

The gel was then transferred to six small beakers for calcination.

16 Collection of calcined CNF samples

The samples were taken out of the calcination oven and they had been calcined successfully with almost no black or grey residue.

The remaining silica was collected in a 4 ml vial and weighed. The mass of the silica was 0.300 g which is enough for the nitrogen sorption analysis.

The sample had a much more brittle and light structure compared to the sample that had the same ratios but consisted of CNC instead of CNF.

50 g SiO_2 [2 wt%] and 50 g CNC [2 wt%] was mixed in a beaker and put to stir for two hours.

The earlier nitrogen sorption analysis samples were ground to prepare them to be run in nitrogen sorption analysis again. They were collected and put back into their respective vial. Sample 1 was the hardest and most difficult to grind while sample 3 was the easiest.

The samples for the calcination were collected using the filtering. The usual calcination method was started. 600°C for 4 hours.

17 Calcination of CNC for nitrogen sorption analysis

Samples collected for calcination.

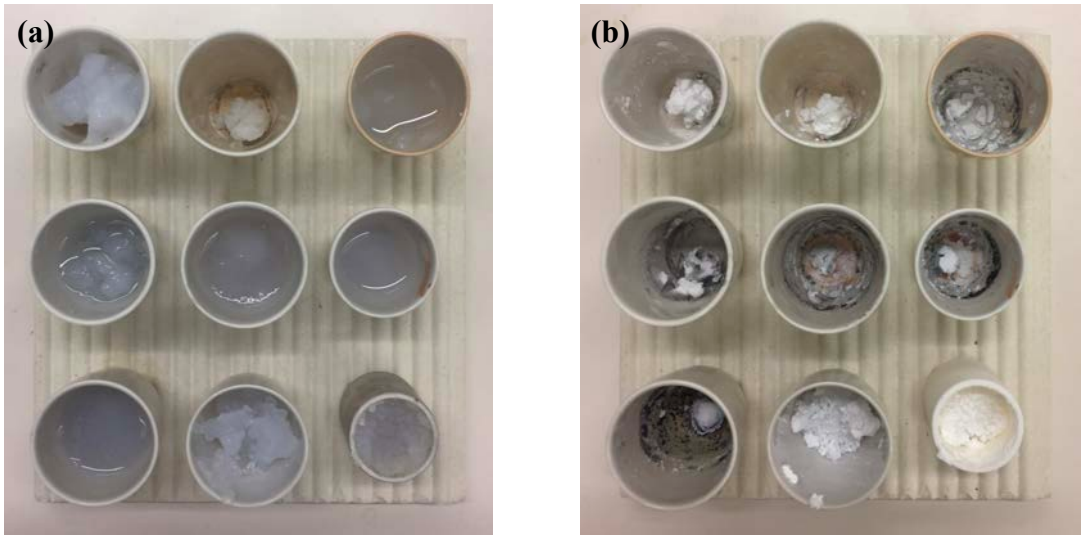

Figure A.3: **(a)** Samples before calcination and **(b)** samples after calcination (600°C).

Row1: 1-2. 79 wt% silica/21 wt% CNC, 3. 50 wt% silica, 50 wt% CNC;
Row 2: 1-2. 21wt% silica 79 wt% CNC 3. 88.24 wt% silica, 11.76 wt% CNC;
Row 3 1. 88.24 wt% silica, 11.76 wt% CNC, 2-3. 99.63 wt% silica, 0.690 wt% CNC

When comparing the samples post and prior to calcination it can clearly be seen that the volume and mass of them has decreased significantly. This is due to the evaporation of the water in the sample and also the calcination in which the cellulose is removed due to the high temperature in the calcination oven (600°C).

The samples that had been calcined were collected from the oven. They were then weighed in a vial. The weight was 0.445 g.

A bit of the sample was grey/black (a sign of not being fully calcined) and that was collected in another vial. The weight for this material was 0.085 g.

The last of the 50/50 SiO_2/CNC was collected from the dish and put into the beakers for calcination at 700°C.

Calcination at 700°C (50/50 SiO_2/CNC).

The beakers with the samples were placed in the oven and set to heat as follows:

0-5 h: 0-700°C, 4 hours at 700°C, 1.5 h cool down period (heating turned off).

Collection of non-calcined samples for SEM

Table A.15: Non-calcined samples for nitrogen sorption analysis.

Sample	SiO2 [wt%]	CNC [wt%]	CNF [wt%]
1	80	20	-
2	50	50	-
3	20	80	-
4	80	-	20
5	50	-	50
6	20	-	80

A 35 g 5 wt% $CaCl_2$ pH 4 solution had to be prepared.

35 g * 0.05 = 1.75 g $CaCl_2$, weighed = 1.75 g
m(total) = 35 g, weighed = 35.03 g

The mixture was set to stir for 20 minutes.
All the samples were gelled in their respective baths and collected.

18 SEM analysis

The first four samples were covered with platinum.

Table A.16: Silica/CNC samples for SEM analysis.

Sample	SiO_2 [wt%]	CNC [wt%]	Calcination at 600°C [h]
1	80	20	4
2	50	50	4
3	20	80	4
4	50	50	8

The non-calcined samples were dried in vacuum at room temperature (21°C) for 4 hours.

1. Non-calcined = 80 wt% SiO_2 20 wt% CNC. It could clearly be seen that this sample did not have the many small pores as the calculated sample of the same (initial) concentration. It could be seen that a big crack was present also in the non-calcined samples. The big crack/voids were not filled with cellulose. The SEM pictures also seem to indicate that all the pores are covered with a thick layer of cellulose. For further analysis of the SEM results please see the discussion section of the report.

19 Fibre spinning at a larger scale

Three different samples were prepared:

Table A.17: Preparation of silica/CNF mixtures for large scale fibre spinning

Sample	wt% CNF (dry)	wt% SiO2 (dry)	m CNF (solution) [g]	m SiO2 (solution) [g]	m (total) [g]	wt% CNF (sample)
1	79	21	20.00	0.0933	20.09	0.3484
2	79	21	12.07	7.95	20.02	0.2110
3	50	50	17.02	3.02	20.04	0.2973

The samples were all homogenised at 7000 rpm using the T 18 digital ULTRA-TURRAX® from IKA for 30 seconds. It was noticed that sample 1 foamed a lot upon homogenisation so to rule out that the sample had been contaminated an identical sample was prepared. The remade sample foamed in the same manner.

The samples were then deaerated under vacuum to get rid of the bubbles that had formed during the homogenising step.

Sample 1 was first spun using a 0.66 ml/min extrusion speed and a 3 m/min collection speed.

The sample was difficult to collect as it broke upon trying to get the fibre out of the gelling bath and up on the collector. The needle was then changed to a smaller one with a diameter of 0.275 mm needle and an extrusion rate of 0.257 ml/min and a slightly increased collection speed of 3.5 m/min.

Upon these changes the fibres could quite easily be collected and they did not break on the collector. The fibres where then dried by leaving the collector in room temperature for 30 minutes. The fibres were intact after drying.

Sample 2 was extruded into the bath but the fibres could not be collected as they broke apart very easily upon trying to pull them out of the bath and onto the collector.

Sample 3 was a bit more collectable than sample 2 was not nearly as collectable as sample 1. The fibres broke somewhat upon the collector almost instantly and even more upon drying almost all the fibres broke apart.